22

Treatment of Breast Cancer Lytic Skeletal Metastasis Using a Model in Nude Rats

Michael Zepp et al.*
Unit of Chemotherapy & Toxicology, German Cancer Research Center, Heidelberg, Germany

1. Introduction

Cancer is a life-threatening disease, not as a result of the primary tumor that can be removed surgically in the vast majority of cases but from its metastatic spread to distant parts of the body. These metastases are often seen as a hopeless end-stage of the cancer disease and at this time only palliative treatments are applied. Some of the most prevalent solid tumors, such as breast-, lung- and prostate cancers, metastasize into the skeleton and cause either osteolytic (destructive) or osteoblastic lesions. Both types are often accompanied by bone pain and increased bone fragility and thus are reason for extended suffering. In breast cancer, bone is the site of first distant relapse and the clinical course of these women is relatively long, with a median survival of 2-3 years (1, 2). Lytic skeletal metastases are present in over 90% of patients who die from breast cancer (3).

Many factors are involved in the pathogenesis of lytic skeletal lesions among which the proteins osteopontin (OPN) and bone sialoprotein II (BSPII) are considered to play an important role. In patients with primary breast cancer, elevated serum BSPII was recognized as prognostic marker of subsequent bone metastasis and was associated with poor survival (4-8). BSPII is a noncollagenous protein of the extracellular bone matrix and a member of the SIBLING (**S**mall **I**ntegrin-**B**inding **Li**gand, **N**-linked **G**lycoprotein) family. The SIBLINGs are mainly clustered on human chromosome 4, and include bone sialoprotein II, osteopontin, dentin matrix protein 1 (DMP1), matrix extracellular phosphoglycoprotein (MEPE) and dentin sialophosphoprotein (DSPP) (12). These proteins are normally expressed in mineralizing tissues of bone and teeth but are also found in different cancers (13). In normal bone, BSPII is expressed by osteoblasts, osteoclasts and other skeleton-associated cell types, especially at sites of new mineral formation (12, 14-16). In this case, BSPII is a potential nucleator of hydroxyapatite formation and a specific marker of osteoblast differentiation (14). The sialoprotein is involved in hydroxyapatite and collagen binding, as well as in the attachment of bone cells including fibroblasts, osteoblasts and osteoclasts to solid surfaces,

* Tobias J. Bäuerle[1], Victoria Elazar[2], Jenny Peterschmitt[1], Rinat Lifshitz-Shovali[2], Hassan Adwan[1], Franz P. Armbruster[3], Gershon Golomb[2] and Martin R. Berger[1]
[1]*Unit of Chemotherapy & Toxicology, German Cancer Research Center, Heidelberg*
[2]*School of Pharmacy, Faculty of Medicine, The Hebrew University of Jerusalem, Jerusalem*
[3]*Immundiagnostik AG, Bensheim*
[1,3]*Germany*
[2]*Israel*

but they are also secreted by breast cancer cells and this presumably is related to their specific homing into osseous tissue (12, 14, 16-19). This fact as well as the interaction with molecules as factor H, integrins, and the ensuing stimulation of signaling cascades promoting migration led to consider BSPII as an important player in the pathogenesis of lytic skeletal lesions (18, 20).

One of the other sibling proteins is osteopontin which is a secreted, adhesive non-collagenous phosphorylated glycoprotein. This molecule was found to be a metastasis-associated protein in human breast cancer in that over-expression of OPN in breast tumours as well as in blood of patients was highly correlated with tumour progression and bad prognosis (21, 22). OPN was initially described as a protein, the secretion of which was elevated in many transformed cells in culture (23). In addition, OPN can bind to a number of receptors such as integrins as well as to certain variant forms of CD44, and it can act as a cytokine (24-26).

For further investigation of the functions from BSPII and OPN in the course of bone metastasis formation, we set up an animal model that would allow following processes such as tumor cell extravasation, adhesion to the target tissue (bone) and formation of osteolytic lesions. For this complex scenario, animal models are indispensable tools to investigate the pathogenesis of bone metastasis *in vivo* and to examine the effects of a therapeutic intervention. For inducing breast cancer bone metastasis in rodents, most experimental models require the injection of human cancer xenografts into immunodeficient mice. This is commonly achieved by intracardial injection or intraosseous administration of breast cancer cells (27). Disadvantageously, the former mode of tumor cell administration into the left ventricle of the heart is associated with dissemination of tumor cells into all skeletal and visceral peripheries of the organism. Local intraosseous administration, however, causes bone damage and lacks processes such as tumor cell extravasation and invasion. Finally, methods based on the injection of bone specific tumor cell subclones are more likely to specifically induce and mimic the process of bone metastasis, but metastatic dissemination is still observed at multiple skeletal sites.

Here we describe a new experimental animal model for inducing site-specific osteolytic lesions in the hind leg of nude rats. This method is characterized by intra-arterial injection of human breast cancer cells into an anastomosing vessel between the femoral and the iliac arteries. This model can be applied to explore the effects of a drug against bone related tumors, which should result in a reduced growth of osteolytic lesions in the treated animals.

2. *In vivo* metastasis model

Nude rats (RNU strain) were obtained from Harlan Winkelmann (Borchen, Germany) or Charles River (Sulzfeld, Germany) at an age of 4–6 weeks. They were housed 4 per cage at specific pathogen-free conditions in a minibarrier system of the central animal facility. Autoclaved feed and water was given ad libitum to the animals that were maintained under controlled conditions (21 ± 2°C room temperature, 60% humidity, and 12 hour light-dark rhythm).

Subconfluent human breast cancer cells (MDA-MB-231^{GFP+}) were harvested using 2 mM EDTA in PBS- (phosphate-buffered saline without Ca^{2+} and Mg^{2+}) and 0.25% trypsin. The cells were washed twice with PBS (with Ca^{2+} and Mg^{2+}), subsequently counted and re-suspended in PBS to a concentration of $5x10^5$ cells per 1 ml. For tumor cell implantation, rats were anaesthetized with a mixture of laughing gas (nitrous oxide; 1 l/min), oxygen (0.5 l/min) and isoflurane (1–1.5 vol. %).

The respective area of a rat's hind leg was shaved and disinfected. A clear cut of 2–3 cm length was performed in the inguinal region (Fig. 1).

Fig. 1. Shaved and desinfected rat thigh, prepared for tumor cell implantation - showing the first incision.

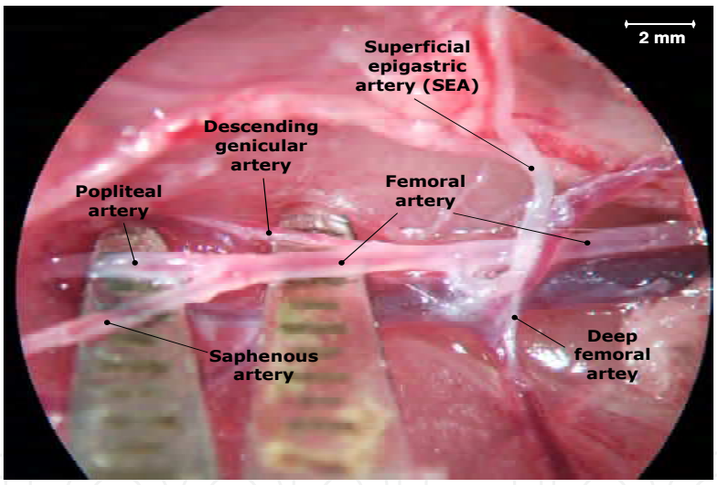

Fig. 2. The branching pattern of the femoral artery, photographed through an operation microscope (magnification 16-fold).

After preparation of all arterial branches as seen in Figure 2, the flow of the femoral artery (FA; Fig. 2) was temporarily occluded by clips that were placed proximal and distal of the superficial epigastric artery's (SEA; Fig. 2) origin. The deep femoral artery (Fig. 2), which normally branches off the FA thus supplying the medial and caudal muscles of the thigh, was also clipped in cases of an anatomical variant as seen in Figure 2. In addition, the SEA was ligated distally, which allowed the opening of this vessel without bleeding. In this context, it is interesting to note that a ligation of the distal SEA is possible because it anastomoses with the caudal epigastric artery that arises from the pudendoepigastric trunk, which is a branch of the iliac artery. After making an incision proximal of the ligation, a 1% papaverin solution was administered onto the SEA to facilitate the subsequent insertion of a

needle (0.3 mm diameter and 42 mm length). After insertion, the needle was fixed in an external support, which reduces irregular movements that would result in perforation of the arterial wall and allows connection with a syringe. Then the distal clip was removed from the FA and placed onto the saphenous artery, which runs superficially and supplies the dorsal and plantar aspects of the foot. MDA-MB-231^{GFP+} cells (10^5 cells suspended in 0.2 ml PBS) were slowly injected into the SEA and by virtue of the clips directed to the descending genicular and popliteal arteries (Fig. 2), both supplying the knee joint and muscles of the right hind leg.

The growth of these tumor cells as well as the formation of lytic lesions was followed subsequently by radiographic examinations. The imaging of the rats was performed every 7 – 14 days under general anesthesia. The animals were fixed in a.p. and p.a. position and exposed to X-rays. The X-ray films were processed by an automatic developing machine and the resulting images were scanned using a digital imaging program with a resolution of 300 dpi. After inverting the scanned radiographs (turning positive into negative), analyses were done with a computer based imaging program. From the beginning to the end of this study, tumor growth and lytic lesions occurred exclusively in the femur, tibia and fibula of the respective hind leg (Fig. 3a). For a 3-dimensional volume rendering reconstructions of the skeleton we performed a high resolution computed tomography (HRCT) using a Multidetector Somatom Plus 4 CT-scanner (based on CT slices with 0.5 mm thickness). Whole animals were investigated with a native spiral scan (Fig. 3b).

2.1 Pilot study

In a pilot study on the optimum take rate, the parameters tumor cell number and sex were varied. For this purpose, male and female animals were observed for a period of 90 days after administering increasing tumor cell numbers. Two male and 2 female rats, respectively, received an injection into the superficial epigastric artery of the right hind leg containing $2.5x10^4$, $7.5x10^4$, $2.5x10^5$ and $7.5x10^5$ MDA-MB-231 or MDA-MB-231^{GFP+} cells.

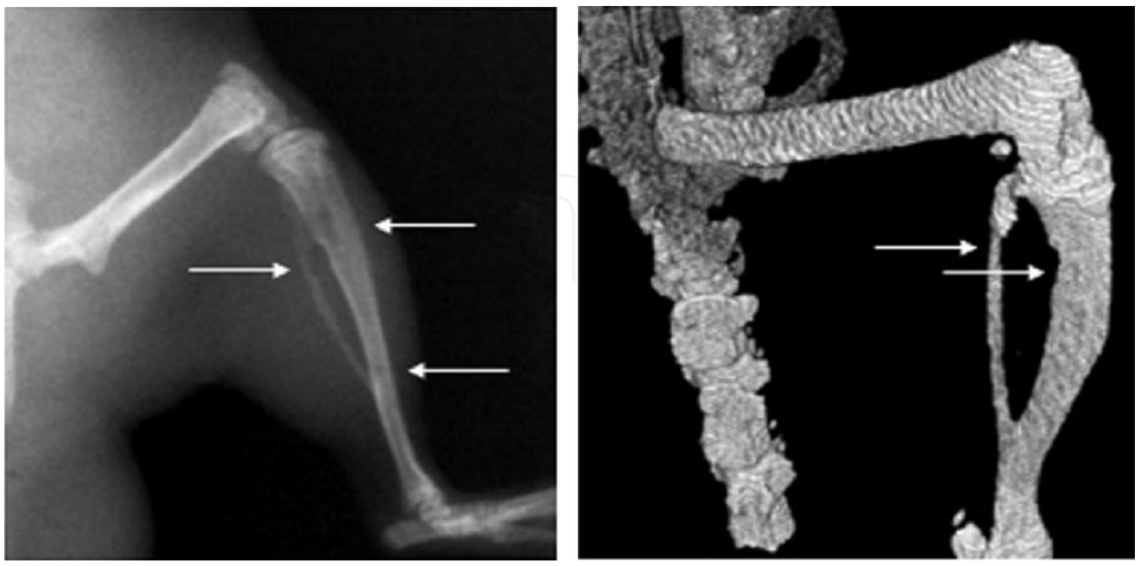

a1) b1)

Fig. 3. (Continued)

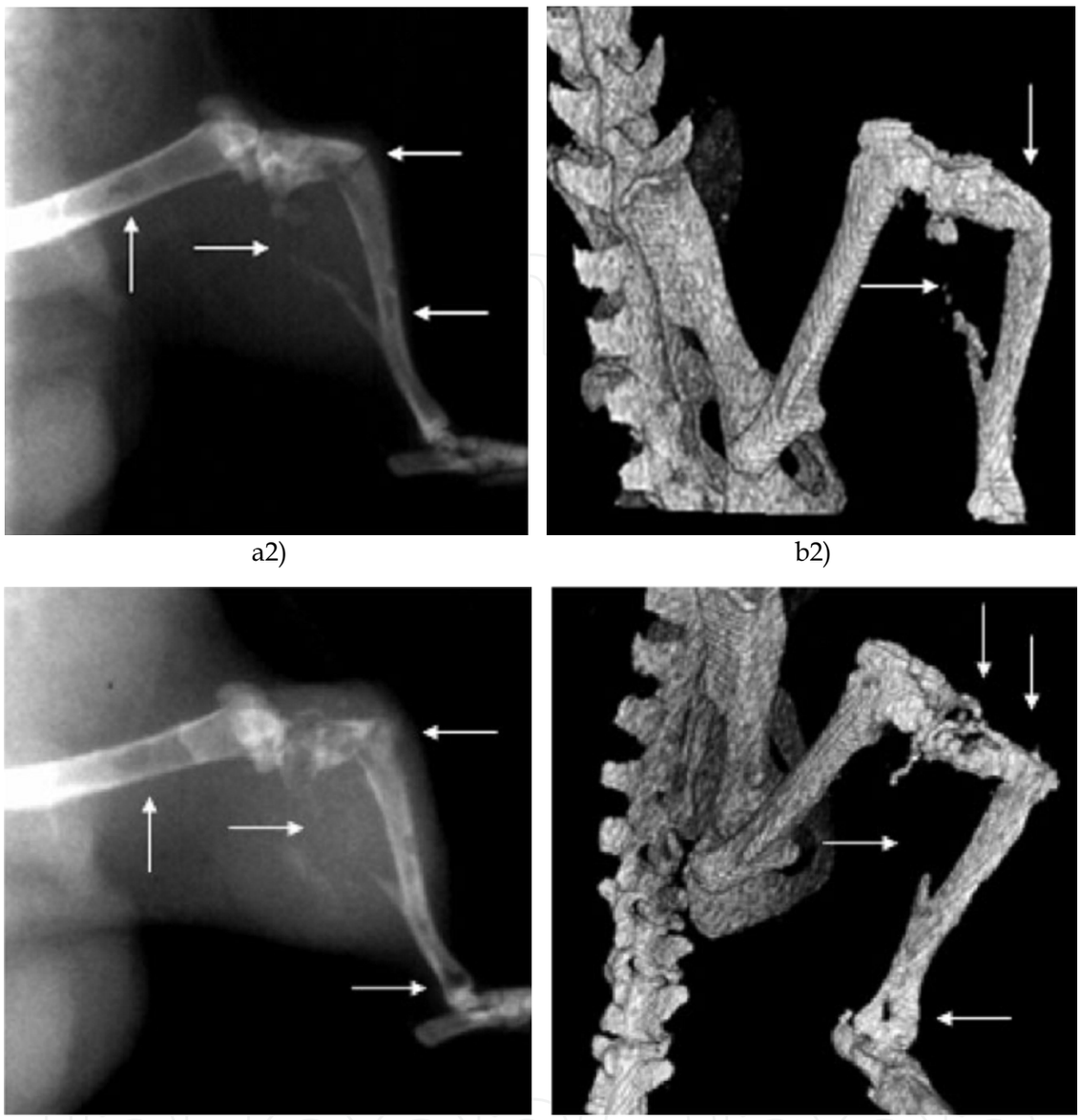

Fig. 3. (a, b) Comparison of the lytic lesions of an untreated control rat detected by 2 radiographic imaging techniques (lesions are indicated by arrows).
(a) X-ray in a.p. position
a1) at day 30 after tumor cell inoculation,
a2) at day 66 after tumor cell inoculation,
a3) at day 104 after tumor cell inoculation.
(b) Computed tomography scan reconstruction
b1) at day 30 after tumor cell inoculation,
b2) at day 66 after tumor cell inoculation,
b3) at day 104 after tumor cell inoculation.

As a result, 50% of all animals developed discernible lytic lesions within an observation period of 90 days. In 5 of 8 males and in 3 of 8 females, overt lytic lesions were observed by

X-rays. The tumor take rate did not differ between MDA-MB-231 and MDA-MB-231^{GFP+} cells (4 of 8 animals, respectively). Cell numbers between 7.5x10^4 and 2.5x10^5 were found appropriate, as these animals developed more and bigger lesions in comparison to rats receiving higher or lower numbers of cells. In an additional group of 7 female nude rats, only 3 developed discernible lytic lesions after inoculation of 1x10^5 MDA-MB-231^{GFP+} cells. Overt lytic lesions were detected by X-rays in some animals as early as 3 weeks after tumor cell implantation. The inoculation of 1x10^5 MDA-MB-231^{GFP+} cells was well tolerated as animals recovered quickly from general anesthesia and did not show weight loss or any signs of walking with a limb.
As a consequence, 1x10^5 MDA-MB-231^{GFP+} cells were inoculated into male rats as basis for all further animal studies.

2.2 Evaluation of the animal metastasis model

By using an amount of 1x10^5 tumor cells the corresponding tumor take rate was 92.7%. In the subgroup of control rats, 2 of 27 (7.4%) showed a spontaneous complete remission of an established lytic lesion within the observation period and 1 rat showed a delayed appearance of its lytic lesion at day 50 after tumor cell inoculation.
The appearance of lesions was usually first detected in the distal femur and the proximal tibia of the hind leg inoculated with tumor cells. Thereafter, small single lytic lesions started to increase in extend and to become confluent with adjacent lesions. Advanced lytic tumor growth was associated with development of surrounding soft tissue metastasis in 8 of 25 rats (32%), and with circular defects of cortical bone in 9 of 25 rats (36%). On average, soft tissue metastasis was detected earlier than circular cortical defects (60 days vs. 80 days after tumor cell inoculation, respectively), and was observed mainly in animals with fast growing lesions of the skeleton. In this rat model, the development of osteolytic lesions can be monitored up to at least 110 days after tumor cell inoculation.

3. *In vitro* experiments for characterization of an IgY antibody

The polyclonal antibodies used were developed in chicken against human bone sialoprotein II and were obtained from the company **Immundiagnostik** (Bensheim, Germany). Appropriate dilutions were made using PBS without Ca^{2+} and Mg^{2+}.
In this part of the study, MDA-MB-231^{GFP+} human breast cancer cells were exposed to an IgY antibody against bone sialoprotein II in order to determine the effect on proliferation, colony formation and migration (Table 1).
Proliferation assay. A volume of 100 µl RPMI medium per well containing 5x10^3 MDA-MB-231^{GFP+} cells was plated onto 96-well plates. After 24h 100 µl medium was added containing the anti-BSPII IgY antibody at final concentrations of 1-400 µg/ml anti-BSPII antibody. The plates were kept under standard cell culture conditions for 1-7 days of incubation. Thereafter, 10 µl/well of 3-[4,5-dimethylthiazol-2-yl]-2,5-diphenyltetrazolium bromide (MTT; 10 mg/ml) was added to determine the number of surviving cells. The supernatant was removed after 3h of incubation, and formazan crystals that had been developed were dissolved by adding of 100 µl acidified 2-propanol/well (0.04 N HCl). Extinction was measured by an automated microtiter plate reader at 540 nm, reference filter 690 nm.
It was found that a concentration below 1 mg/ml medium was ineffective. Higher concentrations gradually decreased cell proliferation with the highest concentration (400 mg/ml) precluding any proliferative activity of MDA-MB-231^{GFP+} cells. The IC50

corresponded to 140 mg/ml at 7 days after start of treatment. Incubation of MDA-MB-231^{GFP+} cells for up to 7 days with concentrations from 1 to 400 µg/ml anti-BSPII antibody decreased the proliferation in a dose- and time-dependent manner as examined by MTT assay. The T/C% value of exposed cells decreased gradually from 101 (1 µg/ml) to 5 (400 µg/ml) after 7 days of incubation (Table 1).

Colony formation assay. For determining the response of MDA-MB-231^{GFP+} cells after exposure to the anti-BSPII IgY, 5x10^5 cells were pre-incubated for 48h in 2 ml RPMI medium containing anti-BSPII at concentrations of 1-400 µg/ml. Thereafter, MDA-MB-231^{GFP+} cells were harvested, counted and transferred into semi-solid medium with 0.8% RPMI-methylcellulose and 30% FBS. Finally, 1 ml of the semi-solid medium containing 5x10^3 MDA-MB-231^{GFP+} cells was plated onto 3.5 cm Petri-dishes. Triplicate Petri-dishes per treatment protocol were cultivated for 5-7 days at standard cell culture conditions. Colony formation (clusters of ≥30 cells) was visualized by staining with MTT and scored by an inverted microscope.

The same range of concentrations as in the MTT assay was chosen to study the colony formation of MDA-MB-231^{GFP+} cells after exposure to the anti-BSPII immunoglobulin. Following 2 days of pre-incubation in medium, colony formation on methyl cellulose was dose-dependently inhibited, with T/C% values ranging from 107 (1 µg/ml) to 17 (400 µg/ml; see Table 1).

Migration assay. In a model for cell migration, 1x10^3 MDA-MB-231^{GFP+} cells were incubated with final anti-BSPII IgY concentrations ranging from 1 to 200 µg/ml. They had been incubated for 48h before being transferred into a transwell migration system. The breast cancer cells were plated on a polycarbonate filter membrane with a pore size of 8 µm (upper layer). The bottom layer was set up by 0.5 ml RPMI medium containing 1x10^4 SaOs-2 cells (osteosarcoma), which were grown in 24-well plates. After 24h the medium was removed and a semi-liquid RPMI medium containing 0.2% methylcellulose and 20% FBS was transferred on top of the SaOs-2 cells (0.5 ml/well) in order to maintain a gradient between the two compartments and to provide an additional barrier for cell migration. The polycarbonate filter was removed from the bottom layer after 24h of co-cultivation and transferred onto a fresh well containing bottom layer (see above). Cells migrating through the pores were counted daily for 4 days by fluorescence microscopy. The mean growth rate (MGR) of cells after migration through the polycarbonate filter was determined by the equation:

$$MGR = \log_2 N_t - \log_2 N_0/t,$$

with N_0 as initial cell number, N_t as final cell number and t as time period of cell incubation in days.

Following pre-incubation for 2 days, MDA-MB-231^{GFP+} cells showed enhanced migration in response to 1 µg/ml anti-BSPII (146 T/C%, day 1). Cells pre-incubated with higher concentrations of anti-BSPII (25-200 µg/ml) showed decreased T/C% values ranging from 92 to 11 (25-200 µg/ml, day 1). This inhibition of migration decreased gradually with time. At day 4 after exposure, only cells pre-incubated with 200 µg/ml anti-BSPII showed significantly reduced migration (59 T/C %) compared to untreated control cells. Cells that had migrated towards the bottom layer were allowed to proliferate for up to three days.

Their mean growth rates (MGR; Table 1) ranged from 0.64 (25 µg/ml) to 0.25 (200 µg/ml), as compared to the MGR of untreated controls (0.80). A control IgY antibody did not show any significant effect (data not shown).

Assay	1 µg/ml	25 µg/ml	50 µg/ml	100 µg/ml	200 µg/ml	400 µg/ml
Proliferation assay[a]	100.9	86.9	77.1	62.7	26.9	5.3
Colony formation assay[b]	106.6	94.2	86.4	54.2	43.2	17.3
Migration assay[c] (MGR)[d]	145.5 (0.72)	91.5 (0.64)	86.6 (0.69)	31.03 (0.32)	10.7 (0.25)	---

[a] Determined by MTT assay; T/C% values after 7 days of incubation with anti-BSPII IgY.
[b] T/C% values of colony counts at day 7 after plating; for treatment the cells were pre-incubated with anti-BSPII IgY for 2 days.
[c] Number of migrating cells in % of untreated control; T/C% values at day 1 after pre-incubation of MDA-MB-231^{GFP+} cells with anti-BSPII IgY.
[d] Mean growth rate (per day): mean of growth rates (day 1/day 2 and day 2/day 3) determined in cells migrating through pores with a diameter of 8 µm; MGR of control: 0.80.

Table 1. Overview of *in vitro* results.

4. Treatment of lytic skeletal metastasis with an anti-BSPII immunoglobulin

The whole *in vivo* study comprised seven groups of nude rats with a total number of 81 animals (Table 2). Untreated control rats (group 1) were observed for a period of 90 days. The effect of the antibody was assessed by either exposing MDA-MB-231^{GFP+} cells prior to their implantation (groups 2 and 3) or by treating rats bearing MDA-MB-231^{GFP+} cells early (group 4) or late (groups 5-7) after tumor inoculation (Fig. 4). Early treatment started at the day of tumor inoculation and additional s.c. injections were given 2 and 4 days later. Late treatment was administered to rats after the appearance of lytic lesions (Fig. 4). Treatment with erucylphospho-NNN-trimethylpropanolamine ($ErPC_3$), used as control, was given i.v. after the onset of lytic lesions (31-34 days following tumor inoculation; group 5, Table 2) for a period of 8 weeks. Treatment with anti-BSPII IgY and the combination consisting of the alkylphosphocholine $ErPC_3$ and anti-BSPII IgY was maintained over the same time period (groups 6 and 7, Table 2). The antibody and $ErPC_3$ were tolerated well without any side effects.

Group no.	Animal no. (% total study)	Mode of treatment	Agent	Concentration/ dosage	Time period of exposure/treatment schedule
1	25 (30.9)[a]	Untreated control rats	---	---	---
2	9 (11.1)	Pre-treatment of cells (HD[b])	Anti-BSPII IgY	600 µg/ml	2h[f]
3	11 (13.6)	Pre-treatment of cells (LD[c])	Anti-BSPII IgY	25 - 100 µg/ml	48h[f]
4	12 (14.8)	Early treatment	Anti-BSPII IgY	20 mg/kg s.c.	Day 0, 2, 4[g]
5	8 (9.9)	Late treatment (APC[d])	$ErPC_3$	60 µmol/kg i.v.	Twice weekly for 8 weeks[h]

Group no.	Animal no. (% total study)	Mode of treatment	Agent	Concentration/ dosage	Time period of exposure/treatment schedule
6	8 (9.9)	Late treatment (AB[e])	Anti-BSPII IgY	10 mg/kg s.c.	Once weekly for 8 weeks[h]
7	8 (9.9)	Late treatment (APC + AB)	$ErPC_3$ + Anti-BSPII IgY	60 µmol/kg i.v. $ErPC_3$ + 10 mg/kg s.c. anti-BSPII	Twice weekly ($ErPC_3$) + once weekly (anti-BSPII) for 8 weeks[h]

[a] Two rats with spontaneous regression were excluded; the initial number was 27.
[b] High dose. [c] Low dose. [d] Alkylphosphocholine. [e] Antibody.
[f] Pre-incubation of MDA-MB-231^{GFP+} cells before tumor implantation.
[g] Three injections of 20 mg/kg were given subcutaneously on days 0, 2 and 4 after tumor implantation. [h] Treatment of rats after the occurrence of lytic lesions.

Table 2. Design of *in vivo* experiments.

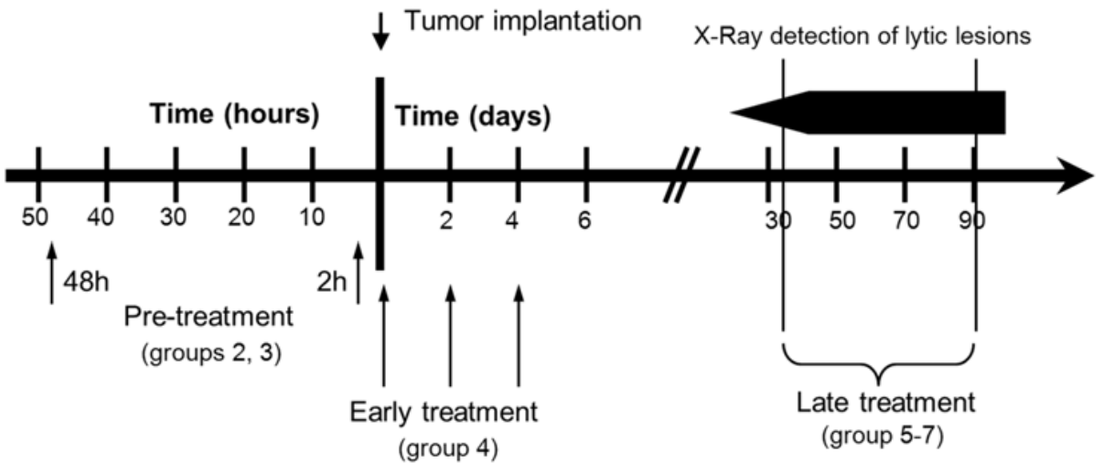

Fig. 4. Time axis of *in vivo* experiment.

In vivo experiments were performed with pre-treated MDA-MB-231^{GFP+} cells, which were incubated with anti-BSPII IgY for 2 days (group 3) or 2 h (group 2) before implantation into nude rats (pre-treatment). Animals of group 4 received the anti-BSPII IgY at the day of tumor implantation, as well as 2 and 4 days later (early treatment). In groups 5-7, treatment was administered to rats with lytic lesions for 8 weeks (late treatment).

4.1 Pre-treatment

The mean lytic lesion size of animals implanted with pre-treated MDA-MB-231^{GFP+} cells increased more slowly and was significantly smaller at days 70-90 than the corresponding mean lesion size of untreated controls (Fig. 5a). One of 11 rats (9%) did not develop any visible metastasis during the observation time of 90 days.

Rats receiving pre-treated cells (groups 2 and 3) showed no circular defects of cortical bone or any soft tissue metastasis surrounding the lytic lesions during the observation time of up to 90 days (Table 3). Untreated control rats developed a circular defect of cortical bone in 9 of 25 rats (36%) and soft tissue metastasis in 8 of 25 cases (32%; Table 3). In comparison to

untreated control rats, the average daily growth rate was distinctly lower in animals receiving pre-treated cells. For animals of group 2, the average daily growth rate was 0.07 mm^2 and for those of group 3 it was negative (-0.01 mm^2). In contrast, lesions of untreated control rats increased by 0.55 mm^2 per day on average.

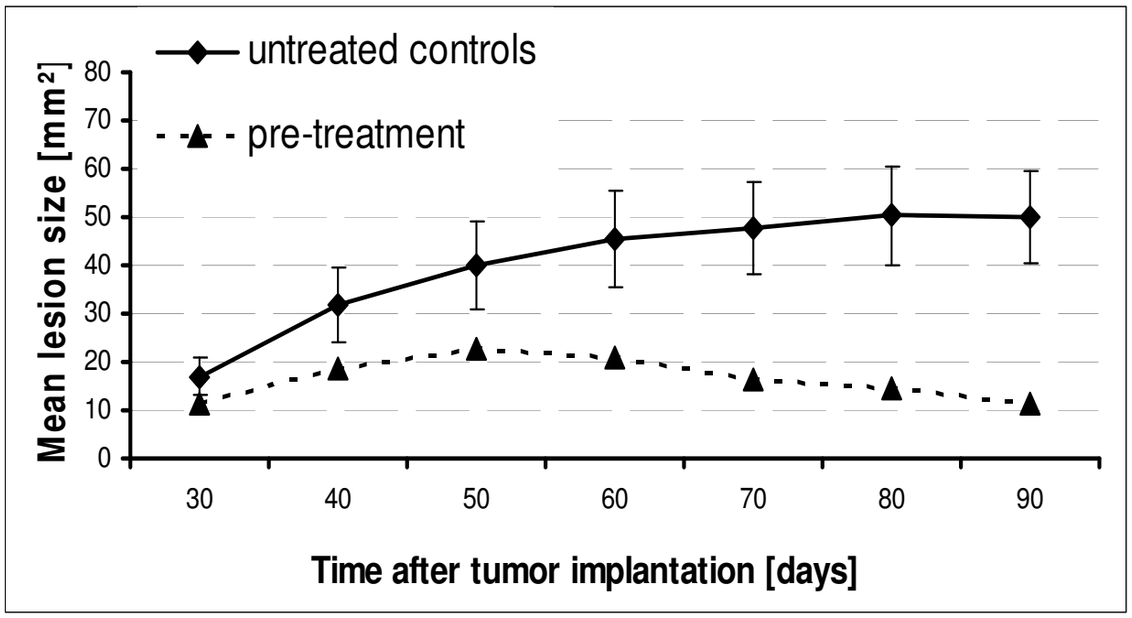

Fig. 5a. Results of *in vivo* experiments. Comparison of the mean lytic lesion sizes of untreated control rats and animals receiving pre-treatment for 48 h (group 3).

4.2 Late treatment

The mean lesion size of animals receiving $ErPC_3$ (group 5, Table 2) increased from day 30 (24 mm^2) to day 60 (63 mm^2) after tumor implantation, and then reached a plateau (Fig. 5b). There was no statistically significant difference to untreated control rats during the observation time. The mean lytic lesion size of animals treated with 10 mg/kg anti-BSPII increased from day 30 (10 mm^2) to day 60 (39 mm^2) after tumor implantation (group 6, Table 2; Fig. 5c). Thereafter, the average lesion size decreased significantly to a minimum size at day 90 (29 mm^2, $p<0.05$) in comparison to untreated controls. The average daily growth rate was 0.32 mm^2 compared to 0.55 mm^2 for the controls (Table 3).

The average lytic lesion size of animals receiving both, $ErPC_3$ and anti-BSPII IgY (group 7, Fig. 5c) increased minimally from 28 mm^2 to 32 mm^2 at day 60 and to 34 mm^2 at day 90 after tumor cell implantation. The average growth per day was 0.1 mm^2 (Table 3). At days 70 and 80, the mean lytic lesion size was significantly smaller than that of untreated control animals (30 mm^2 and 26 mm^2, $p<0.05$). Animals receiving late treatment with the antibody alone or in combination showed fewer complications such as circular bone lysis or soft tissue metastasis caused by the growth of lytic lesions in comparison to untreated control rats (Table 3).

The suitability of the anti-BSPII antibody for a combination therapy was tested by co-administering the antibody with the alkylphosphocholine $ErPC_3$. This agent has been shown to reduce proliferation, colony formation and migration in MDA-MB-231^{GFP+} cells *in vitro*. In nude rats with bone metastasis, this drug alone caused no reduction in lytic lesion size,

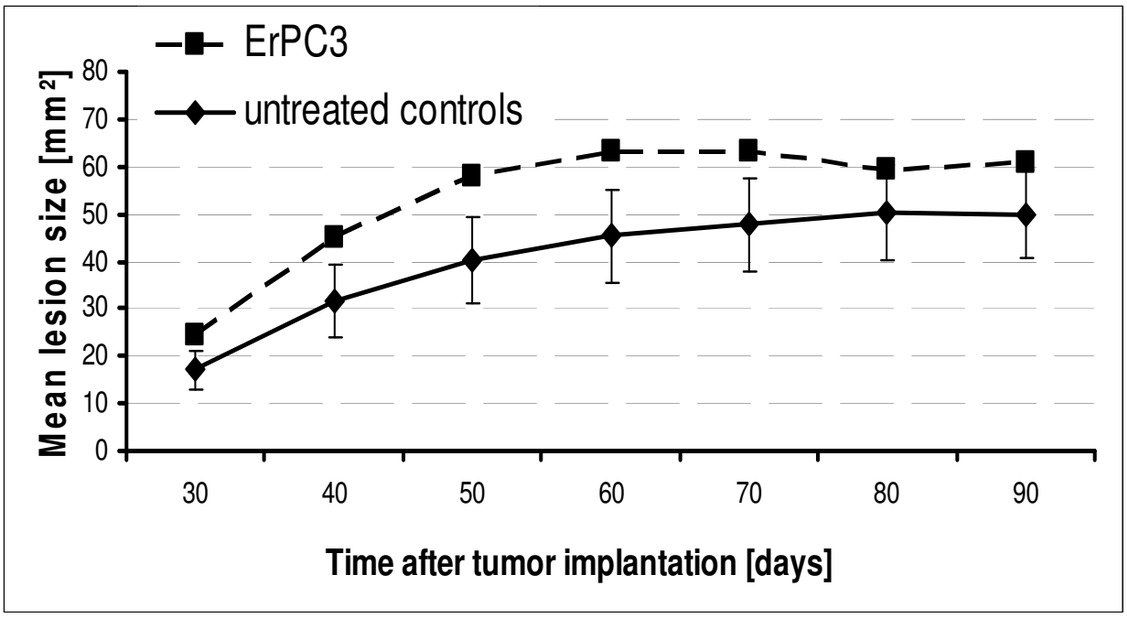

Fig. 5b. Results of *in vivo* experiments: Comparison of the mean lytic lesion sizes of untreated control rats and animals receiving late treatment with $ErPC_3$ (group 5).

but the combination with anti-BSPII IgY resulted in a significant decrease in mean osteolytic lesion size. Also, new bone formation was observed in rats treated with anti-BSPII IgY + $ErPC_3$. This *de novo* bone formation resulted in almost complete remissions of lytic lesions as well as in stabilization of pathologically fractured bones in some rats (Fig. 6, Line VII c, d).

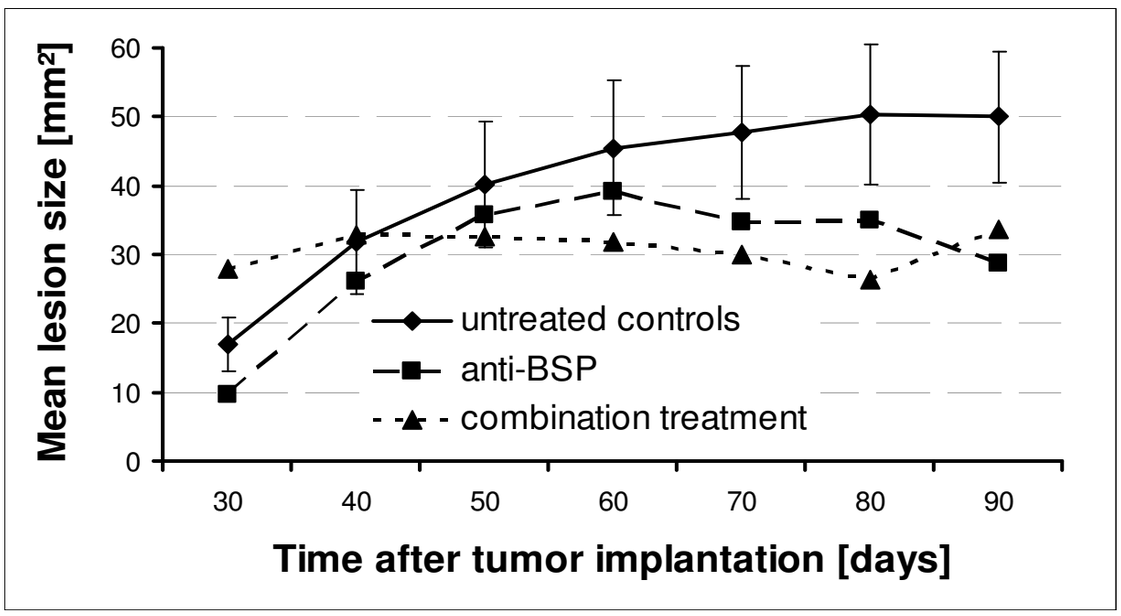

Fig. 5c. Results of *in vivo* experiments. Comparison of the mean lytic lesion sizes of untreated control rats and animals receiving the anti-BSPII IgY alone (group 6) or in combination with $ErPC_3$ (group 7).

Parameter observed	Group 1	Group 2	Group 3	Group 4	Group 5	Group 6	Group 7
T/C% [a] (day 30)	100	37,.6[b]	67.2[b]	48.6[b]	143.1	56.1	164.1
T/C% [a] (day 60)	100	18.7[b,f]	45.7[b]	29.9[b,f]	138.7	86.1	70.3
T/C% [a] (day 90)	100	[c]	28.8[b.f]	[c]	118.6	69.6	52.5 [f]
T/C% [a] (day 90)	100	[c]	22.4[b,f]	[c]	121.2	57.3 [f]	67.5
Rats with circular defects of cortical bone (%)[d]	9 (36)	0 (0)[f]	0 (0) [f]	0 (0)[f]	3 (37.5)	2 (25)	2 (25)
Rats with soft tissue metastasis (%)	8 (32)	0 (0)[f]	0 (0) [f]	0 (0) [f]	3 (37.5)	2 (25)	1 (12.5)
No. of rats without visible metastasis (%)/	---	1 (11.1)	1 (9.1)	2 (20)	---	---	---
No. of complete remissions (%)	2 (7.4)	---	---	---	2 (25)	1 (12.5)	0 (0)
Average daily growth rate of lytic lesions[e] (day 30-90) (mm^2)	0.55	0.07 [f]	-0.01 [f]	0.18f	0.61	0.32 [f]	0.10 [f]

[a] Mean lytic lesion size of experimental rats in percent of the corresponding lesion size of untreated controls. [b] Mean value excluding rats without any visible metastasis.
[c] Group terminated at day 60 after tumor implantation.
[d] Circular defects of femur or tibia potentially resulting in a bone fracture; circular defects of the fibula were excluded.
[e] Average daily growth rate from day 30 to 90 after tumor implantation for groups 1, 3, 5-7 and from day 30 to 60 for groups 2 and 4. [f] Significant difference versus control rats ($p<0.05$).

Table 3. Results of *in vivo* experiments.

Consequently, reduced osteolytic lesion sizes were observed in rats that had been treated with the antibody against BSPII before or after the appearance of skeletal metastasis. Beyond that, in rats with overt lytic lesions, at days 60 - 65 new bone formation was observed in the femur and tibia. On computed tomography reconstructions (Fig. 6) of this animal, the new bone formation in response to anti-BSPII treatment can be seen with greater plasticity. Remarkably, formation of new bone has previously not been described after treating overt osteolytic lesions. Even bisphosphonates being the most widely used treatment for patients with breast cancer bone metastasis are only able to delay the growth and progression of skeletal lesions by inhibiting osteoclast-mediated bone resorption.

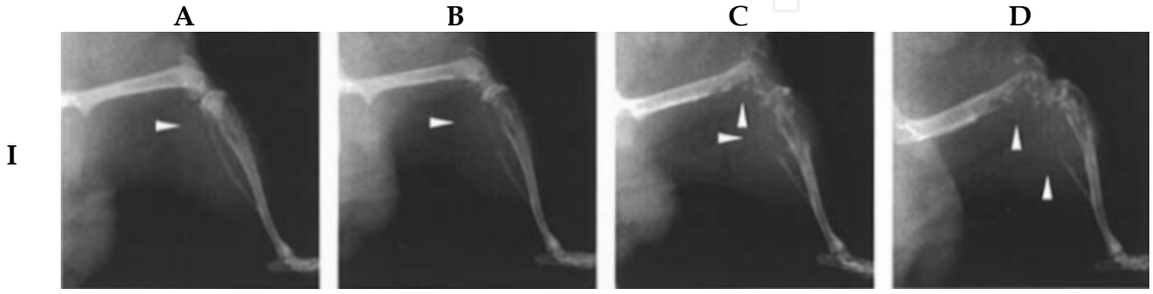

Fig. 6. (Continued)

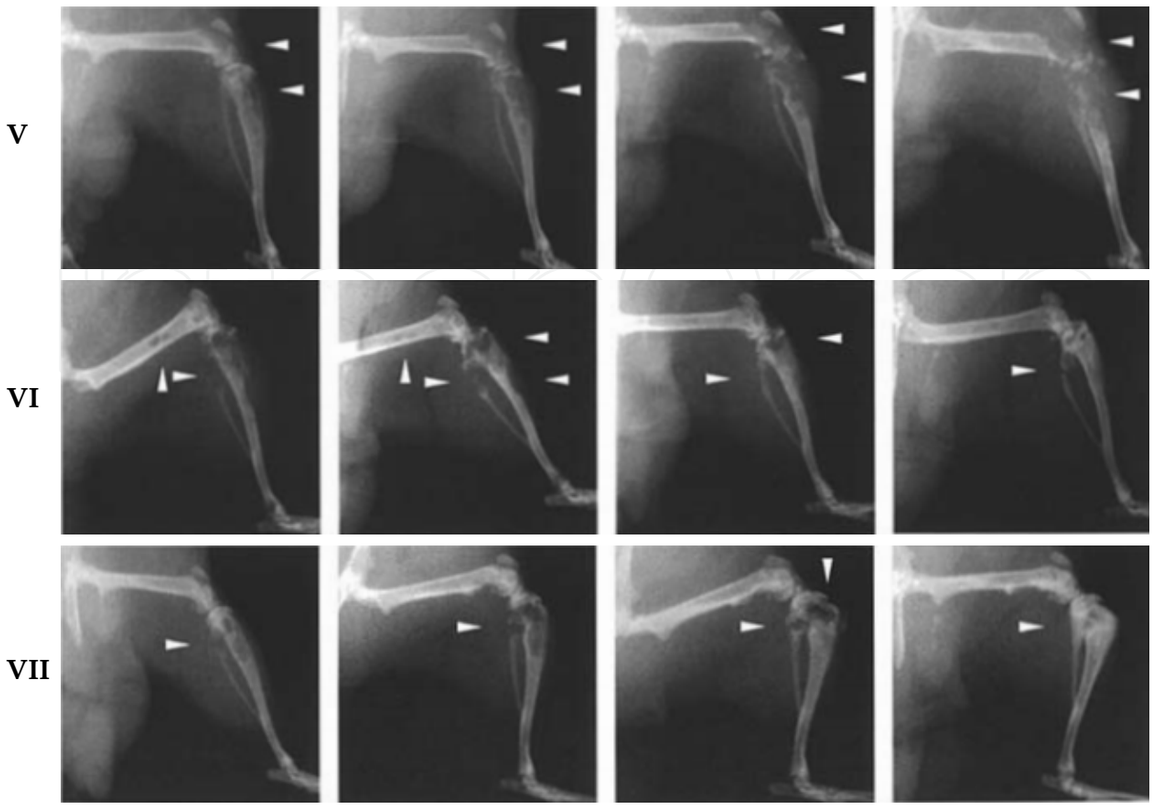

Fig. 6. Radiographic comparison of lytic lesions in the right hind leg of nude rats (lesions are indicated by arrows). Serial X-rays of experimental rats taken after 30-35 days (A), 40-45 days (B), 60-65 days (C) and 80-95 days (D) after tumor cell implantation.
Roman numbers denote individual animals, they correspond also to their group numbers and these rats are typical for the whole group. These include an untreated control rat (I, group 1), a rat (V) treated with $ErPC_3$ (group 5), a rat (VI) treated with anti-BSPII IgY antibody, and a rat (VII) treated with $ErPC_3$ plus the IgY antibody (group7).

5. Combination treatment of lytic skeletal metastasis with the bisphosphonate zoledronate and the anti-BSPII IgY

Over the last decades, bisphosphonates have become an essential part of the treatment of bone metastasis. They bind with high affinity to hydroxyapatite crystals and therefore accumulate in the skeleton. There they are potent inhibitors of osteoclast bone resorption and thus prevent or reduce the development of osteolytic lesions caused by breast cancer cells (28). Besides this established efficacy, N-containing bisphosphonates have been shown to inhibit the activity of farnesyl diphosphonate synthase, a key enzyme in the mevalonate pathway (29). In addition, these third generation bisphosphonates have been shown to exert cytostatic and pro-apoptotic effects on breast cancer cells *in vitro* (30). Nevertheless, treatment with bisphosphonates is considered as a palliative measure and therefore various drug combinations have been examined to improve the overall anti-neoplastic effect in breast cancer patients with skeletal metastasis (31-33). Among various options that can be envisaged the combination with an agent targeting the pathophysiology of skeletal lesions seems therapeutically attractive.

In addition to these studies demonstrating that an IgY-antibody against BSPII was effective in reducing proliferation, colony formation and migration of MDA-MB-231^{GFP+} cells *in vitro* as well as *in vivo* it could be shown that this treatment induced new bone formation in the aforementioned nude rat model (34, 35).

Therefore it was the aim of this study to combine a potent bisphosphonate, e.g., zoledronic acid, with the IgY antibody for treating the mammary carcinoma cell line MDA-MB 231^{GFP+}, which causes osteolytic lesions *in vivo*. The combination of agents with unrelated mechanisms of action was expected to result at least in an additive combination effect.

In order to explore a possible synergistic effect in lytic skeletal metastasis caused by MDA-MB-231^{GFP+} cells, the rats were treated with combined exposure to zoledronic acid and the IgY antibody against bone sialoprotein II alone or in simultaneous combination.

The experimental design is shown in Table 4. An untreated control group (group 1) was compared with five different treatment groups. The untreated control group was monitored radiographically over a period of 100 days after tumor cell inoculation. A possible preventive effect of zoledronic acid was tested on a group of ten rats (group 2) by administering 60 µg/kg (150 nmol/kg) subcutaneously on days 14 and 7 prior to tumor cell inoculation. This group was examined over a period of 70 days following tumor cell inoculation. Furthermore, zoledronic acid alone was used in an early treatment scheme prior to the development of lytic lesions (group III; n = 10; 60 µg/kg/week [150 nmol/kg/week] zoledronic acid, s.c.; d7-d28 after tumor cell injection) as well as in combination with the anti-BSPII IgY (group IV; n = 10; 60 µg/kg/week (150 nmol/kg/week) zoledronic acid, s.c.; d7-d28 after tumor cell injection plus 20 mg/kg anti-BSPII IgY, s.c.; d1, d3, d5 after tumor cell injection). These groups were also examined over a period of 70 days.

In addition, two groups of rats (n = 10 each) with established lesions were treated according to a late treatment scheme. One of these groups (group V) received a late single drug treatment (60 µg/kg/week [150 nmol/kg/week] zoledronic acid, s.c.; d35–d84 after tumor cell inoculation) and the other group (group VI) was treated with a late combination treatment (60 µg/kg/week [150 nmol/kg/week] zoledronic acid, s.c.; d35–d84 after tumor cell inoculation and 10 mg/kg/week anti-BSPII IgY, s.c.).

Group no.	Animal no. (% total study)	Mode of treatment	Agent	Concentration/ dosage	Time period of exposure/ treatment schedule
1	20 (28.57)	Untreated control rats	---	---	---
2	10 (14.28)	Pre-treatment of rats	zoledronic acid	60 µg/kg/week s.c.	Day 14, 7 before cell inoc.
3	10 (14.28)	Early single treatment	zoledronic acid	60 µg/kg/week s.c.	Day 7, 14, 21, 28 after cell inoc.
4	10 (14.28)	Early combination treatment	zoledronic acid + Anti-BSPII IgY	60 µg/kg/week s.c. 20 mg/kg s.c.	Day 7, 14, 21, 28 after cell inoc. Day 1, 3, 5 after cell inoc.[a]
5	10 (14.28)	Late single treatment	zoledronic acid	60 µg/kg/week s.c.	Once weekly during 35d-84d[b]
6	10 (14.28)	Late combination treatment	zoledronic acid + Anti-BSPII IgY	60 µg/kg/week s.c. 10 mg/kg s.c.	Once weekly during 35d-84d following cell inoc.

[a] before the appearance of lytic lesions. [b] after the appearance of lytic lesions.

Table 4. Design of *in vivo* experiments.

5.1 Pre-treatment

The mean lytic lesion size in animals receiving preventive treatment was significantly smaller than the mean lesion size of untreated controls at days 30–60. The increase in size of existing lesions was significantly lower (average daily growth rate: 0.3 mm^2/d vs. 45.3 mm^2/d) as compared to untreated controls. The incidence of lesions was significantly reduced to 50%. Soft tissue metastases occurred in 20% (2/10) of rats which corresponds to half the incidence observed in untreated control rats (8/20; 40%). The significant reduction in lesion size was corroborated by analyzing the manifestation of lesions in the involved skeleton. Lesions in the femur and fibula were reduced by 55 and 65%, respectively, whereas lesions of the tibia were present in each animal affected. Also, the number of rats with periosteal defects of the cortical bone was significantly smaller as shown by a 60% incidence in the treated group versus 95% in the control group (Table 5).

5.2 Early treatment

The mean lesion areas of the early single drug and combination treatment schedules were almost identical. The initial mean lytic lesion areas were significantly smaller than the respective control area (4.0 and 4.8 mm^2 vs. 25.6 mm^2). Remarkably, the respective T/C% values of 15.5 and 18.6 at day 30 decreased with time to 5.5 and 6.5 at day 60. The average daily growth rate (mm^2/d) was significantly reduced from 45.3 mm^2/d in controls to 0.2 mm^2/d in animals receiving single drug treatment and to 0.1 mm^2/d in those receiving the combination treatment. The incidence of lytic lesions was significantly reduced to 30% with both early treatment schemes corresponding to a 70% reduced incidence as compared with the control group. Periosteal defects of cortical bone were prevented totally with the early combination treatment and were reduced to 33% with the early single drug treatment. The appearance of lytic lesions was decreased by both early treatment schemes in the femur and fibula, the latter being significant ($P \leq 0.05$). Soft tissue metastasis was not observed following the single drug treatment whereas the combination treatment was associated with a reduced incidence of 20% compared to 40% in the control group (Table 5).

5.3 Late treatment

With both late treatment schemes the mean lesion areas were significantly reduced as measured at 60 and 90 days following tumor cell inoculation. The late combination treatment improved the effect of zoledronic acid. For example, the mean lesion area at day 60 following tumor cell inoculation was 93.5 mm^2 in the control group, 31.3 mm^2 in the late single drug treatment group and 19.5 mm^2 in the late combination treatment group. The average daily growth rate of lytic lesions significantly decreased from 45.3 mm^2/d (control group) to 0.3 mm^2/d (late single drug treatment group), and to 0.2 mm^2/d (late combination treatment group) after 60 days following tumor cell inoculation and from 22.7 mm^2/d (controls) to less than 0.01 mm^2/d (single drug treatment) and 0.05 mm^2/d (combination treatment) after 90 days following tumor cell inoculation. The remission rate of lytic lesions was significantly increased to 40% (single drug treatment) and 30% (combination treatment) compared to the control group (5%, $P = 0.015$ and $P = 0.057$, respectively). The appearance of lytic lesions was reduced in all affected bones (femur, tibia and fibula) with both late treatment schemes. For lesions of the femur and fibula the combination treatment was slightly more effective than zoledronic acid alone, reaching almost significance ($P = 0.06$) for lesions of the femur. Similarly, the development of periosteal defects of cortical bone was significantly reduced in all three bones ($P < 0.05$) except for the femur following treatment

with zoledronic acid. Here, the late single drug treatment caused a reduction by 35% whereas the late combination treatment reduced this parameter by even 55%. In both late treatment groups just half as many rats developed soft tissue metastasis as compared to the control group (Table 5).

The clinical dose of zoledronic acid in oncology is 4 mg i.v. every 3 – 4 weeks, which corresponds to about 110 µg/kg. Thus, a single experimental dose corresponded to about 60% of a single clinical dose. When considering total dosages, the preventive regimen with a total of 120 µg/kg administered in two weeks is within the clinical range given within 3 – 4 weeks. The early and late treatment regimens summed up to 240 and 480 µg/kg within 4 and 8 weeks, respectively. These doses are about two fold higher than the equivalent clinical doses (4 and 8 mg within 4 and 8 weeks, respectively). Of note, the experimental doses are even lower than the clinically used doses if they are compared on the basis of body surface area. In this case the rats received single doses of about 0.4 mg/m² body surface area as compared to 2.2 mg/m² in patients. The corresponding total doses in rats were 0.8 mg/m² (pre-treatment), 1.6 mg/m² (early treatment) and 3.2 mg/m² (late treatment). The latter value is to be compared to 4.4 mg/m² in the clinical situation for a period of 8 weeks. Thus, overall the dosages used in rats were equivalent to those in patients although tumors usually grow faster in rats than in humans. Therefore the single doses were given more frequently in rats in order to produce relevant results.

The antiosteolytic effect of zoledronic acid in nude rats was only marginally increased by the IgY antibody. The therapeutic advantage was best discernible in the incidence of femoral osteolytic lesions when comparing zoledronic acid alone (80%) with the combination treatment (40%), but was less pronounced when comparing periosteal defects of cortical bone (60% vs. 40%). The main difference to the *in vitro* design was a lower dose of zoledronic acid in vivo (60 µg/kg) which already caused a maximum therapeutic effect and thus this effect could not be improved significantly by addition of the IgY antibody. A reason for this observation could be the pharmacokinetic property of bisphosphonates to accumulate in bone. The affinity of bisphosphonates for bone has been correlated with a long half-life and is similar to that observed for tetracyclines, strontium or fluoride. Thus, the skeletal concentration of zoledronic acid, together with its potency, was presumably too high to allow survival of the majority of osteoclasts and therefore caused the maximum antiosteolytic effect possible. In this scenario the IgY antibody could only show additional activity if it exerted a direct tumoricidal action or a stimulatory effect on osteoblasts. Both properties have been demonstrated in previous studies. Since zoledronic acid has tumoricidal properties as well, a clear difference between zoledronic acid and the combination would be hard to identify. Therefore, we hypothesized that a direct effect on osteoblasts may be the basis for the differences favoring the combination that were seen in response to the late treatment groups.

It is unclear why the combination effect could best be observed in the femur of the animals. Recently, it has been described that osteolytic lesions induced by human MDA-MB-435 breast cancer cells in nude mice were associated with a greater than 90% reduction in the number of osteoblasts. Based on this observation we speculate that the size of osteolytic lesions might be indicative for the extent of this effect, in that smaller lesions might be associated with a lower reduction in osteoblast counts as opposed to larger lesions. In that case those bones with initially smaller or less frequent osteolytic lesions such as the femur could be left with a higher number of osteoblasts which would be able to recalcify osteolytic lesions upon appropriate stimulation.

Observed Parameter		Time period (day)[a]	Controls	Pre-treatment (Zoledronic acid)	Early treatment		Late treatment	
					Zoledronic acid	Combination	Zoledronic acid	Combination
Mean area (mm^2) ± SD		30	25.6 ± 10.8	5.3 ± 4.1*	4.0 ± 2.8*	4.8 ± 4.0*	23.3 ± 18.7	12.9 ± 13.6
		60	93.5 ± 52.8	13.7 ± 8.2*	5.1 ± 3.2*	6.1 ± 5.8*	31.3 ± 32.3*	19.5 ± 19.7*
		90	106.2 ± 57.3				23.4 ± 25.7*	15.6 ± 15.8*
growth rate of lytic lesions (mm^2/d)[b]		30–60	45.3	0.3*	0.2*	0.1*	0.3*	0.2*
		30–60	22.7				≤ 0.01*	0.05*
Incidence of lytic lesions		30–60	100% (20/20)	50% (5/10)*	30% (3/10)*	30% (3/10)*	100% (10/10)	100% (10/10)
Rate of lytic lesions remission[c,d]		30–60	5% (1/20)	0% (0/5)	0% (0/3)*	0% (0/3)*	40% (4/10)*	30% (3/10)*
Distribution of lytic lesions	Femur	30–60	75% (15/20)	20% (1/5)*	33% (1/3)	33% (1/3)	80% (8/10)	40% (4/10)
	Tibia	30–60	100% (20/20)	100% (5/5)	100% (3/3)	100% (3/3)	90% (9/10)	90% (9/10)
	Fibula	30–60	85% (17/20)	20% (1/5)*	0% (0/3)*	0% (0/3)*	70% (7/10)*	60% (6/10)*
Rats with circular defects of cortical bone	Total	30–60	95% (19/20)	60% (3/5)*	33% (1/3)*	33% (0/3)*	60% (6/10)*	40% (4/10)*
	Femur	30–60	50% (10/20)	0	0	0	40% (4/10)	10% (1/10)*
	Tibia	30–60	85% (17/20)	60% (3/5)	33% (1/3)	0	50% (5/10)*	30% (3/10)*
	Fibula	30–60	80% (16/20)	0	0	0	30% (3/10)*	30% (3/10)*
Rats with soft tissue metastasis		30–60	40% (8/20)	20% (2/10)	0	20% (2/10)	20% (2/10)	20% (2/10)

[a] Days following tumor cell inoculation. [b] Average daily growth rate.
[c] Percentage based on all animals that were observed only or treated after the occurrence of lytic skeletal lesions. [d] Remission = Decrease in size ≥ 50% of initial size. *Significant effect versus control ($P \leq 0.05$).

Table 5. Effect of administering zoledronic acid alone and in combination with anti-IgY BSPII treatment.

In conclusion, the combination of zoledronic acid and the anti-BSPII antibody caused only a low therapeutic advantage over zoledronic acid alone, probably due to a maximum anti osteolytic effect caused by the bisphosphonate alone. Nevertheless, an almost significant effect was observed in parameters indicating recalcification such as the reduction of osteolytic lesions and the prevention of periosteal defects of cortical bone. These observations may favor using the IgY-antibody in addition to zoledronic acid in order to stimulate osteoblast induced recalcification.

6. Treatment of lytic skeletal metastasis with antisense oligonucleotides against OPN and BSPII

Here, we report on the selection of antisense oligonucleotides (ASOs), which are effective in reducing their protein levels. We considered the two proteins to be potential targets for treatment in order to slow down or suppress the formation of bone metastasis. For a specific treatment, we identified antisense oligonucleotides that are capable of reducing the expression levels of OPN and BSPII. The activity of these ASOs was determined by Western blot and by inhibition of colony formation as well as of metastasis formation of pre-exposed MDA-MB-231^{GFP+} human mammary carcinoma cells (36, 37).

Selection of ASOs

The suitability of 10 different ASOs per gene was predicted by using the HUSAR program ''Mfold'', which takes RNA folding into account. Application of this program onto the cDNA sequence of OPN (acc. no. gi:3360431) and BSPII (acc. no. gi:11435526) resulted in the recognition of RNA stretches that probably contain bulges or loops, that are preferentially single stranded and thus allow access of DNA antisense structures. ASOs of 20 base pair length were selected against these single-stranded regions and synthesized with a phosphorothioate backbone, to increase stability against degrading enzymes (Table 6). Controls included a nonsense oligonucleotide (NSO) derived from the HBV genome that served as a control for unspecific effects of a 20 bp long phosphorothioate oligomer. In addition, its base composition differed only slightly from the mean composition of all ASOs used (A:3 versus 4.1; C:4 versus 4.4; G:6 versus 4.8; T:7 versus 6.6). Sequence-specific effects were controlled by using ASOs differing by three base pairs with regard to the respective cDNA sequence. Finally, the use of 10 ASOs per target gene allowed to include sequences that were scrambled (identical in base composition) except for two bases that were permutated.
For determining the potential secretion of OPN and BSPII, an MDA-MB-231^{GFP+} subline was generated, which was selected by continuously reducing the FBS content of the medium, until the cells kept growing without FBS. This cell line was denoted as MDA-MB-231^{F}. All cells were kept in log-phase, and passaged 1 – 3 times per week depending of their growth rate, and maintained under standard conditions (37°C, humidified atmosphere, 5% CO_2).
Stock solutions of ASOs in distilled water were diluted to appropriate concentrations with phosphate-buffered saline (PBS). For transfecting cells with ASOs, lipofectamine (Lipofectin, Invitrogen, Karlsruhe, Germany) or electroporation was used.

$ErPC_3$

For treating MDA-MB-231^{F} cells, $ErPC_3$, which was kept as stock solution in ethanol and PBS (10mM; ratio of diluents 1:1; V:V), was diluted in PBS resulting in final concentrations of 10, 14 and 20 mM. The medium containing $ErPC_3$ was changed after 24 hours in all experiments and the cells were further grown for 48 – 72 hours without $ErPC_3$ (for details of sequential exposure see below).

No.	(OPN)[a] cDNA	(BSPII)[a] cDNA
ASO-01	bp 73–92	bp 46–65
	5'-CTC ATG GTA GTG AGT TTT CC-3'	5'-TGA TTG CTT CCT CTG GCA GT-3'
ASO-02	bp 661–680	bp 53–73
	5'-TTC AGG TCC TGG GCA ACG GG-3'	5'-ATT TTG GTG ATT GCT TCC TC -3'
ASO-03	bp 662–681	bp 328–347
	5'-GTT CAG GTC CTG GGC AAC GG-3'	5'-CTT CAT TGT TTT CTC CTT CA-3'
ASO-04	bp 1343–1362	bp 331–350
	5'-CTA ACT TAA AAA ACA AAA GA-3'	5'-ATT CTT CAT TGT TTT CTC CT-3'
ASO-05	bp 1346–1365	bp 505–524
	5'-ACA CTA ACT TAA AAA ACA AA -3'	5'-CTT CAT CAC TTT CCT TCT CT-3'
ASO-06	bp 193–212	bp 546–565
	5'-GTG GCC ACA GCA TCT GGG TA -3'	5'-GCT TTC TTC GTT TTC ATT TC-3'
ASO-07	bp 193–212	bp 706–725
	5'-GTG GCC ACA GCA TCT GGG TA-3'	5'-TTC CGG TCT CTG TGG TGT CT-3'
ASO-08	bp 195–214	bp 711–730
	5'-ATG TGG CCA CAG CAT CTG GG-3'	5'-CTG CCT TCC GGT CTC TGT GG -3'
ASO-09	bp 556–575	bp 1003–1022
	5'-GGT CTG CGA AAC TTC TTA GA-3'	5'-ACT GGT GGT GGT AGT AAT TC-3'
ASO-10	bp 559–578	bp 1005–1024
	5'-TCA GGT CTG CGA AAC TTC TT-3'	5'-TCA CTG GTG GTG GTA GTA AT-3'

The following sequence from HBV was used as a nonsense control (NSO): 5′-GCG AGG GAG TTC TTC TTC TA-3′. [a]The combination of the abbreviation of the gene and the number of a given ASO was used for its naming.

Table 6. Selected antisense oligonucleotides against OPN and BSPII.

Electroporation

Pending on the duration of treatment, $5x10^5$ – $3x10^6$ cells were suspended in 1ml RPMI 1640 medium without phenol red containing 10 mM concentrations of the respective ASO or NSO. For transfection, the cells were pulsed two or three times for 2ms at 450 or 350V, respectively, in an 800 ml cuvette using an electroporation impulse generator (EPI2500, Dr L Fischer, Heidelberg, Germany) with the capacitance set at 1200 mF. Thereafter, the cells were plated onto six-well plates and grown for 48 – 72 hours.

Lipofectamine

Pending on the duration of treatment, $1x10^5$ – $3x10^5$ cells were transferred onto six-well plates and grown for 24 hours. For transfection, ASO stock solutions were prepared in medium without FBS. According to the protocol of the manufacturer, the respective ASO stock solution was mixed with lipofectamine to allow ASO–liposome complexes to form. To 200 ml medium containing ASO quantities resulting in 10 mM (Western blot and in vivo model) and in 5, 10, or 20 mM (clonogenicity assay) final ASO concentrations, an equal volume of medium without FBS was added containing 5, 10 or 20 ml lipofectamine, respectively. In addition to the ASO treatment, an NSO control (20 mM final concentration with 20 ml lipofectamine) and a lipofectamine control (20 ml) were used. Based on the equilibrium of the ASO–liposome complex formation, the relatively low amount of

lipofectamine used resulted in effective ASO concentrations that were at least by a factor of 10 lower than those in the medium used for transfection. After 12 hours the medium was changed, and cells were further grown for 48 – 72 hours. In the case of a sequential combination treatment this first cycle was repeated with the respective combination partner.

Combination treatment

Sequential combination treatment consisted of two or three treatment cycles. The two-cycle treatment started either with the ASO and was followed by $ErPC_3$ or was performed with the reverse sequence. The three-cycle treatment started either with two cycles of ASO followed by $ErPC_3$ or an initial exposure to $ErPC_3$ was followed by two cycles with an ASO.

Verification of the ASOs treatment by Western blotting

Transfected cells were incubated, harvested and washed. Thereafter $2x10^6$ cells were counted and prepared for Western blotting. The protein concentration of the lysate was determined using the BCA protein assay from Pierce (Rockford, IL) according to the manufacturer's recommendation. After the cell lysates were separated by electrophoresis and transferred to a PVDF membrane, the membrane was incubated with the respective first antibody (OPN: rabbit–antihuman polyclonal or mouse–antihuman monoclonal antibody; BSPII chicken–antihuman or rabbit–antihuman polyclonal (all from Immundiagnostik, Bensheim, Germany)). An HRP-conjugated anti-mouse, anti-rabbit or anti-chicken secondary antibody (all from Immundiagnostik, Bensheim, Germany) and ECL (Amersham Biosciences, Freiburg, Germany) were used to detect the respective proteins by exposing the membrane to an X-ray film. To control for variations in loading, the membranes were stripped for 30 minutes at 56°C in stripping solution. Thereafter, they were reprobed with an antibody against β-actin (mouse monoclonal antibody, Santa Cruz.CA), and a secondary goat anti-mouse polyclonal antibody (Santa Cruz.CA).

Target protein	**OPN**			**BSPII**		
Type of exposure	Single[a]	Twofold[a]	Single[a]	Single[b]	Single[a]	Twofold[a]
ASO-01	25	34	45	78	58	16
ASO-02	45	60	38	94	94	---
ASO-03	32	38	97	44	93	---
ASO-04	16	23	73	55	109	---
ASO-05	43	80	27	63	101	49
ASO-06	45	68	33	16	79	19
ASO-07	31	69	58	25	37	22
ASO-08	48	97	62	34	101	25
ASO-09	---	74	35	46	84	---
ASO-10	---	86	33	40	30	---
NSO	99.5	99	100	99	100	97
Control	100	100	100	100	100	100

[a] Transfection with lipofectamine. [b] Transfection with electroporation.
The used cell line was MDA-MB 231^F. X-ray films documenting chemoluminescence bands were scanned, digitized bands of the respective protein were expressed in relation to untreated control (100%).

Table 7. Inhibition of OPN and BSPII expression in MDA-MB 231^F cells following exposure to a series of antisense oligonucleotides.

The X-ray films were automatically processed and scanned by using an imaging program. The digitized bands of the respective proteins were given as percent of control and corrected for differences in loading by referring to the intensity of the β-actin band. The Western blot results of protein expression after exposing mammary carcinoma cells to ASOs directed against OPN and BSPII mRNA are shown in Table 7. Systematic comparisons showed that ASO-OPN-04 and ASO-BSPII-06 were the most effective structures within the respective series. Single exposure of cells was enough to reduce the OPN expression by 84% in response to ASO-OPN-04. This effect was not increased by repeating the ASO exposure, but the protein concentration was kept at a comparable level (77%). A similar efficacy was obtained for ASO-BSPII-06, which caused an 84% reduced bone sialoprotein II expression following single exposure and an 81% reduced protein level following two-fold exposure.

In vivo model

In order to induce loco regional bone metastasis, and to investigate a preventive effect of the ASOs, $1x10^5$ MDA-MB 231^F cells (control or pre-exposed to ASOs) were injected into a branch of the femoral artery of a nude rat, as described above. After an average of 28 days following the inoculation of control cells, lytic metastases could be detected by X-rays. The size of these lesions, which exclusively occurred in the femur, tibia and fibula of the animals, was recorded for up to 10 weeks.

The results of the *in vivo* experiments are shown in Table 8. Exposure to the ASO-OPN-04 and ASO-BSPII-06 for 3 days before implantation into nude rats caused a significantly reduced tumor take rate, as assessed by the appearance of osteolytic lesions following exposure to ASO-OPN-04, and a reduced size of osteolytic lesions in the X-ray-positive rats following both agents.

Group no.	Animal no.	Agent[a]	Observation period (weeks)	Incidence of metastasis	Size of lesion[b]	Mean	T/Cx100[c]
1	4	ASO-OPN-04	4	1/4	0, 0, 0, 34	8.5(717)[d]	3.9
			6	1/4	0, 0, 0, 46	11.5(723)	3.8
			8	1/4[e]	0, 0, 0, 60[f]	15(730)	4.3
2	4	ASO-BSPII-06	4	1/4	0, 0, 0, 14	3.5(77)	1.6
			6	1/4	0, 0, 0, 35	8.8(718)	2.9
			8	2/4	0, 0, 20, 106[f]	31.5(751)	9.1
3	2	NSO	4	2/2	106, 240	173(134)[g]	78
			6	2/2	162, 411	287(249)	95
			8	2/2	242, 728	485(486)	140
4	2	Untreated cells control rats	4	2/2	314, 127	221(187)	100
			6	2/2	386, 218	302(168)	100
			8	2/2	425, 266	346(159)	100

[a] MDA-MB-231^F cells were exposed to ASOs or NSO (transfected with lipofectamine), before transplantation to nude rats. [b] Product of pixel number and mean black intensity in individual rats as determined by image analysis from the X-ray radiograph. [c] Mean lesion size of treated over control rats times 100. [d] Numbers in brackets denote SD. [e] P = 0.0028 vs. control groups 3 and 4.
[f] P = 0.05 vs. control groups 3 and 4. [g] Numbers in brackets denote range.

Table 8. Results of in vivo experiments.

Nude rats that received 1x10^5 untreated or NSO-treated MDA-MB-231^F breast cancer cells developed bone metastasis in four of four cases (Table 8). The metastatic lesions were detectable for the first time after 4 weeks and were nearly doubled in size until week eight. Three of four rats that received 1x10^5 MDA-MB-231^F breast cancer cells pre-treated with the ASO, directed against OPN, developed no discernible metastasis within the observation period (P=0.028). One of the four rats developed lytic metastasis, but this lesion was distinctly smaller in size than those in control rats (week 4; P=0.05). Similarly, two of four rats that received 1x10^5 MDA-MB-231^F breast cancer cells pre-treated with the ASO directed against BSPII remained free of visible metastasis within the observation period of 8 weeks; one rat showed lytic metastasis after 4 weeks already, another rat developed a metastasis after 8 weeks. Thus, exposure to both, ASO-OPN-04 and ASO-BSPII-06, was associated with a significantly reduced lesion size, and the former agent caused a significantly reduced incidence of lesions, as well.

7. Biodistribution and efficacy of polymeric nanoparticles containing OPN and BSPII antisenses in a mammary carcinoma rat model

The initial steps in metastasis include invasion of tumor cells into normal tissue, traversion of small blood vessel walls and thus access to the circulation (38). Cancer cells that survive these initial steps can enter the sinusoids of the bone marrow and migrate across the sinusoidal wall to the endosteal bone surface (39). For homing into the bone compartment, tumor cells have to develop specific functions that differ from those in the normal tissue and they presumably express several proteins that assist in this process (40). Osteopontin and bone sialoprotein II, have both been characterized as promising targets for a therapy by antisense oligonucleotides directed against the RNA of these proteins, thus preventing or reducing lytic skeletal metastasis (36, 37). Efficient and specific delivery of antisenses (ASOs) and a protection of the sequences from degradation are the crucial conditions for ASO therapeutic efficiency. Due to their large molecular size and high negative charge density, the resulting low cellular permeability of ASOs is a major problem encountered with their therapeutic use (41-43). To improve cellular delivery of ASOs several methods, employed in DNA delivery, have been developed including viral vectors, liposomes, and other delivery systems (44-46).

Especially one of these nanocarrier systems, the nanoparticles (NP), has been increasingly employed as drug delivery devices of small molecules and particular nucleic acids (47). The nanocarriers are utilized to protect molecules from biodegradation as well as to modify their pharmacokinetics and biodistribution (48).

It was hypothesized that effective and safe ASO delivery could be achieved by polymeric nanoparticles (NP) fabricated from the biocompatible and biodegradable PLGA. Poly(lactic-co-glycolic acid) copolymers (PLGA) are among the few synthetic biocompatible biodegradable polymers approved for human gene therapy use (49). Due to their nano-size range and small negative charge, polymeric nanospheres containing ASOs can overcome the absorption barrier of the cell membrane by penetrating inside the cell *via* endocytosis (50, 51). Moreover, the controlled release delivery mode offers increased resistance to nuclease degradation, sustained duration of ASO administration, and consequently, prolonged antisense action.

In this section we report about the characteristics and therapeutic efficiency of a controlled release nanoparticle (NP) delivery system for ASO sequences, designed against OPN and BSP II. The ASO-NP efficiency in the inhibition of metastatic bone lysis was evaluated in the rat animal model of mammary carcinoma (52, 53).

ASO NP preparation and characterization

A double emulsion system and the solvent evaporation technique were used to incorporate OPN-ASO sequences in PLGA (53). At the end of production finished NP were lyophilized and the dry NP were stored in a vacuum desiccator at 4°C. The amount of ASO entrapped in the NP was analyzed and determined using the fluorescence "Oligreen assay kit" (Molecular Probes, Eugene, OR) and by UV spectroscopy at λ = 260 nm.
NP size and morphology were evaluated by dynamic light scattering, ALV (NIBS/HPPS GmbH, Langen, Germany), and a transmission electron microscope (TEM CN12, Philips, Eindhoven, The Netherlands). Average size and size distribution of empty NP and NP loaded with ASO sequences were measured before and after lyophilization. A zeta-sizer (Malvern Instruments Ltd, UK) was used for evaluation of NP charge (Tab. 9).
Several types of NP have been prepared for the various studies, empty NP (blank, serving as control), NP loaded with NS (control), NP containing OPN or BSPII ASO (ASO-NP); and fluorescent NP including, NP loaded with FITC-ASO (FITC-NP), fluorescent empty NP (PLGA-rhodamine, Rhodamine-NP), and double labeled NP (ASO-FITC and PLGA-rhodamine).

	Size distribution (nm)			Loading	
NP content	**Before lyophilization**	**After lyophilization**	**Surface charge (ζ potential, mV)**	**Yield (%)**	**Concentration (μg AS/mg polymer)**
OPN[a]	234 ± 72	281 ± 85	3.06 ± 0.84	51 ± 9	4.80 ± 0.68
BSPII[b]	236 ± 73	294 ± 98	3.88 ± 0.74	55 ± 14	4.56 ± 1.07
NS	233 ± 70	280 ± 90	2.37 ± 0.47	49 ± 13	6.91 ± 2.82
Empty	291 ± 85	324 ± 104	2.6 ± 0.06	---	---

Mean ± SD, each batch was measured in triplicate. [a]OPN = ASO-OPN-04 and [b]BSPII = ASO-BSPII-06 (Tab. 6)

Table 9. The physicochemical properties of AS NP examined.

7.1 Biodistribution pilot study in healthy rats

In a pilot study we tried to clarify the distribution of the nanoparticles in the organism (rat). Therefore the ASO-OPN-04 sequence (Tab. 6) was internally labeled with ^{33}P (54).
The used rats were randomly assigned to treatment or control groups. Naked ASO-OPN-04 (n = 4) or ASO-OPN-04-NP (n = 5) were injected into a rat tail vein at average $13.2x10^6$ DPM/rat. Rats injected with saline were used as a control group (n = 2). The rats were kept in metabolic cages and their excrements were collected every day. The animals were euthanized 24 h, 72 h, and 7 days post-injection. One milliliter of blood, 0.5 ml of urine, whole organs, samples of skeletal muscles, and feces were taken from each rat for analysis. The radioactivity (DPM = disintegrations per minute) in the samples was counted by means of a liquid scintillation analyzer (Packard, Tri-carb 2900TR, USA) against a calibration curve of $R^2 = 0.986$. The radioactivity was normalized to the animal weight and an organ accumulation was expressed as a percentage of total injected doses (Fig. 7a-c).
Following the above experiment in certain tissues a quantitative examination of the whole body biodistribution was performed comparing naked and NP encapsulated ASO.
Levels of naked ASO increased considerably in most tissues after 24 h, reaching highest values in the liver and spleen. Naked ASO was also found at higher levels in blood, in

comparison to NP encapsulated sequences (9.3 ± 1.0% and 7.7 ± 1.2% naked ASO vs. 3.2 ± 0.5% and 1.9 ± 0.4% ASO-NP after 24 h and 72 h, respectively), but the naked ASO amount was insignificant (0.3 ± 0.0%) after 7 days, when ASO-NP level in blood started to increase (4.0 ± 0.9%). Throughout the time-course of the study, ASO-NP was distributed mainly in the liver and spleen. The total recovery from these two organs was as much as 46.4 ± 3.0% and 74.2 ± 7.4%, 24 h and 72 h after the treatment, respectively, and slightly decreased to 59.3 ± 8.9% after 7 days. In contrast, naked ASO sequences accumulated in the spleen to a much lower extent (2.8% ± 0.4% after both 24 and 72 h, and 1.6% ± 0.1% after 7 days). Although relatively high amounts of naked ASOs reached the liver during the first half of the study (33.8% ± 1.7% and 26.7% ± 4.8%, after 24 and 72 h, respectively), only 8.1% ± 1.4% were found in this organ after 7 days (Figure 7c). Throughout the study naked ASOs accumulated to a small extent in the thymus (2.8% ± 0.9%, 3.8% ± 4.8%, and 1.8% ± 0.3% after 24 h, 72 h, and 7 days, respectively). Relatively low levels of ASO, both naked and NP

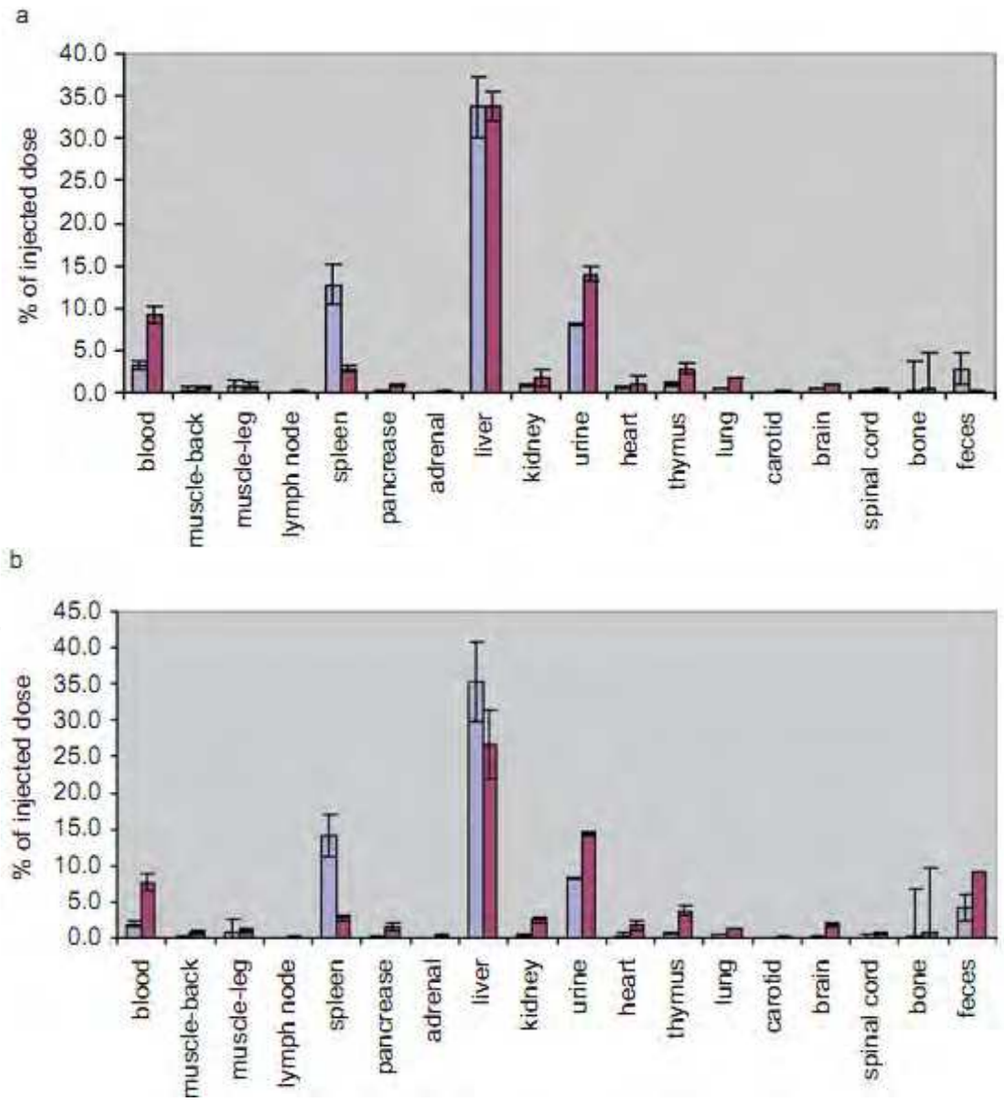

Fig. 7. (Continued)

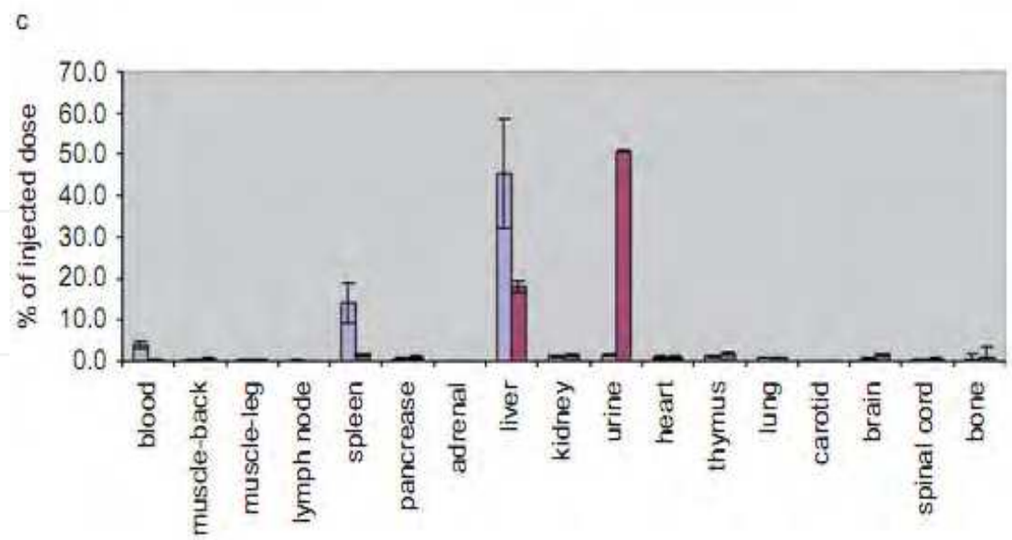

Fig. 7a-c. The quantitative biodistribution of ASO-NP in whole body organs.
Naked (n = 4) or NP (n = 6) encapsulated sequences were internally labeled with ^{33}P ATP and were injected into a healthy male rats (350–400 g) tail vein (average 13.2×10^6 DPM/rat). Rats injected with saline were used as the control group (n = 2). Biodistribution was evaluated 24 h (a), 72 h (b), and 7 days (c) after treatment by beta-counter analysis of blood, organs, and excrement samples. The radioactivity was normalized to the animal weight and organ accumulation was expressed as a percentage of total injected dose (mean ± SD). Bars: blue – ASO NPs, red – naked ASO.

encapsulated, were found in the kidneys at all time points, but always the amount of naked ASO in the kidneys was higher than that of NP encapsulated sequences (1.7% ± 1.0%, 2.5% ± 0.3%, and 1.4% ± 0.3% naked AS vs. 0.8% ± 0.1%, 0.5% ± 0.1%, and 1.2% ± 0.2%, ASO-NP after 24 h, 72 h, and 7 days, respectively). At all time points of the experiment, the accumulation of NP encapsulated ASO was negligible in other organs harvested. Mostly ~1% or less of the injected dose was found in the skeletal muscles, lymph node, pancreas, adrenals, brain, spinal cord, heart, and lungs. Naked ASO was taken up by those tissues to a higher extent than ASO-NP.

Naked ASO and ASO-NP had different clearance profiles. Throughout the study course naked ASO was excreted mainly and rapidly in urine, due to the highly hydrophilic nature of the ASO and its degradation products. Already after 7 days more than half of the naked ASO dose injected was cleared in the urine. In contrast, ASO-NP was excreted in the urine to a lower extent, and a significant amount was also found in the feces at all time points. After 7 days, the clearance of ASO-NP was mostly in feces, whereas only a small ASO amount was found in the urine. The divergent clearance suggests different degradation rate and extent of naked and encapsulated ASO. Following the treatment with naked ASO, all the sequences can be rapidly degraded and cleared in urine. In ASO-NP formulation only the released ASO is exposed to degradation, but encapsulated ASOs remains intact and generally can be found in tissues or excreted in the feces. Moreover, most of the encapsulated ASO was released inside the cells, because of the rapid cellular uptake of NP; hence it is less exposed to degradation by nucleases existing in the extracellular matrix.

It can be concluded that ASO-NP protects the ASO from degradation and provides efficient ASO delivery to the tumor tissue. Moreover, administration by the NP delivery system minimizes ASO accumulation in intact organs due to the ASO sustained release profile, and the favorable NP physicochemical properties.

7.2 NP effects on cells *in vitro*

NP effect on cells' viability

HeLa cells (1.5 x 10^4/chamber) were seeded in a Lab-Tek chambered cover glass system and incubated for 24 hr. The cells were treated with empty NP (10 mg/ml) and were incubated for 24 or 48 hr. At each time point, the cells were washed with PBS and harvested. The total cells' number and amount of living and dead cells were counted, using a hemocytometer. Trypan blue was used for staining dead cells. Non-treated cells were used as a control group. The percentage of living and dead cells was calculated. Statistical differences between NP treated and non-treated groups were tested at each time point by the one-tailed unpaired Student's test. Differences were considered statistically significant at $p < 0.05$.
The average cells' number (living and dead) was similar in treated and non-treated groups 24 hr after treatment (living cells, 95.0% and 96.3%; and dead cells, 5.0% and 5.2% in NP treated and non-treated groups, respectively), as well as after 48 hr (living cells, 94.8% and 95.6%; dead cells, 5.2% and 4.4% in NP treated and untreated groups, respectively).

In vitro visualization of cellular uptake

The cellular uptake of fluorescent ASO sequences encapsulated in rhodamine-labeled PLGA-NP by HeLa and MDA-MB-231 tumor cells was examined. MDA-MB-231 and Hela cells (1.5 x 10^4/chamber) were seeded in a Lab-Tek chambered cover glass system (Nunc International Corp.) and incubated for 24 hr. Fluorescent NP loaded with FITC-ASO or naked FITC-ASO sequences were added to the cells and incubated for 4, 24 or 48 hr.
After methanol fixation the cells were mounted with fluorescence microscopy mounting media. ASO-NP uptake in comparison to naked AS was observed and recorded by means of confocal microscopy (Zeiss LSM 410, Germany). Nontreated cells and cells incubated with empty NP were determined as background. Confocal cross-sections of cells taken at 24 and 48 hr after treatment were used to verify intracellular (cytoplasmic) localization of the NP and the ASO.
Empty fluorescent NP were shown to internalize and accumulate in the cytoplasm of both HeLa and MDA-MB-231 cancer cells, reaching maximal uptake within the first 24 hr (figure not shown). No significant auto-fluorescence was observed in HeLa cells chosen for further uptake evaluation experiments. Similarly to the empty NP, ASO loaded NP were internalized by the cells and accumulated in the cellular cytoplasm. High NP internalization was achieved by 24 hr. In contrast, naked ASO uptake was decreased overtime. Confocal cross-section images of HeLa cells 24 and 48 hr after treatment with ASO-NP verified cell internalization and cytoplasm localization of the NP.
Cells treated with empty NP exhibited a relatively high uptake of 13.6 ± 0.01% already after 4 hr, followed by a gradual increase and thus reaching maximum uptake after 24 hr (44.02 ± 0.68%), and a slight decrease after 48 hr (39.65 ± 0.02%). Treatment with naked ASO resulted in a significant uptake (17.18 ± 0.83% of the cells) already 4 hr after treatment. The naked ASO internalization rate increased to its maximum level after 24 to 48 hr (35.22 ± 19.19% and 30.40 ± 0.11%, respectively). In spite of a relatively rapid NP internalization, fluorescent

signal from FITC-ASO encapsulated in NP was detected in less than 10% of the cells after 8 hr. In contrast, the number of cells loaded with ASO was markedly increased after 24 hr, reaching 58.81 ± 25.75%.

Extent and intensity of NP endocytosis: The representative experiments demonstrate the continued uptake over time of ASO-NP. After 24 hr, a significant increase of NP uptake was exhibited in cells treated with empty rhodamine-NP. ASP-NP internalization (encapsulated FITC ASO) was also observed after 4 hr, but to a lesser extent than naked ASO. In contrast, the fluorescence of FITC-ASO in NP was markedly increased after 24 hr, and was much higher than that of naked ASO. Internalization of naked ASO was significant already after 4 hr (41.48 ± 0.03). The AS accumulated inside the cells, reaching 63.22 ± 0.01 and 74.45 ± 0.11, after 24 and 48 hr, respectively. In contrast, empty NP uptake was slower, 21.12 ± 0.01 after 4 hr, increasing gradually to 46.43 ± 0.01 after 24 hr. The uptake of rhodamine-NP was decreased after 48 hr. Following treatment with ASO encapsulated in non-fluorescent NP, relatively low levels of ASO were detected inside the cells after 4 and 8 hr, increasing significantly after 24 hr (150.25 ± 0.87).

7.3 Bioactivity – Inhibition of metastatic bone lysis by OPN and BSPII ASOs

The tumor cells were inoculated as described above (see chapter 2). Resulting bone metastases and their mean lytic lesion size was followed by X-ray examinations once weekly for 12 weeks. Treatment results were observed in groups of 4–5 rats at each arm of the studies. The lesion size was measured from X-ray pictures using image analysis software, and the mean lesion size and lesion ratio (mean lesion size in treated group in percent of control) were calculated. The mean lesion size was presented in relative units (RU), corresponding to the image analysis of the pixel's count.

The results were expressed as mean ± SD. Statistical differences between groups in the metastatic lesion size were assessed by the one way ANOVA test.

The treatment with NP, loaded with ASOs (OPN or BSPII), was administered immediately after tumor inoculation into the same vessel as the cells (superficial epigastric artery, Fig. 2). The amount of NP (100 mg in 500 μl PBS, total dose of 600 μg of NSO or ASO) was divided: two thirds of the dose was injected into the vessel and one third (using the same needle) was injected loco regionally, into the muscle surrounding the knee joint (in order to avoid clogging of the artery).

The inhibition of metastatic bone lysis by OPN and BSPII ASO-NP was evaluated in a rat mammary carcinoma metastasis model. Most animals treated with nonspecific NSO delivered by NP (4 of 5 rats) developed bone metastasis (Tab. 10) and multiple lesions in the femur, tibia and fibula. The metastatic lesions were detectable for the first time after 4 weeks (mean lesion size of the control group, 16 ± 14 RU, doubled in size until week 8 (38 ± 36) and continued to grow in all rats till the end of the experiment (week 12).

Treatment with OPN ASO and BSPII ASO loaded NP resulted in a significant decrease in tumor bone metastasis incidence, as assessed by the reduced appearance of osteolytic lesions (Table 10) and in a reduced size of the lesions in metastasis-positive rats. Two of the 4 rats developed lytic metastasis following the treatment with OPN NP, and 3 of 5 with BSPII NP, but the lesions in the ASO NP treatment groups were distinctly smaller in size than those in the control group of NSO-NP (Table 10). Both ASO sequences successfully prevented metastasis incidence and even caused tumor regression in most animals; 3 of 4 and 3 of 5 animals were found free of visible metastasis at the end of the

observation period (week 12) following the treatment with OPN and BSPII NP, respectively (Table 10). It was found that the BSPII ASO had a response by the inhibition of metastasis, but it was somewhat less effective than OPN ASO in bone lysis reduction, when delivered by NP.

Treatment type	Time (weeks)	Metastasis incidence (tumor bearing rats / animals)	Mean lesion size[1]	Lesion ratio T/C x 100[2]
NSO[3]	4	4 / 5	16 ± 14	100
	6	4 / 5	38 ± 36	100
	8	4 / 5	56 ± 62	100
	10	4 / 5	72 ± 81	100
	12	4 / 5	85 ± 97	100
ASO-OPN-04	4	2 / 4*	7 ± 8	44
	6	2 / 4*	9 ± 12	24
	8	2 / 4*	11 ± 18	20
	10	1 / 4*	7 ±13	9
	12	1 / 4*	4.5 ± 9	5
ASO-BSPII-06	4	3 / 5	9 ± 8	56
	6	3 / 5	17 ± 17	45
	8	3 / 5	20 ± 22	36
	10	3 / 5	14 ± 17	19
	12	2 / 5*	12 ± 18*	14

[1] Product of pixel number and mean black intensity (±SD) in individual rats as determined by image analysis from the X-ray radiograph.
[2] Mean lesion size of treated over control rats x100.
*Statistically significant vs. control group (χ^2 test), $p < 0.01$.
[3] Nonsense oligonucleotide (NSO) were used as control group.

Table 10. Inhibition of metastatic bone lysis by OPN and BSPII antisenses delivered by nanoparticles.

It may be concluded that ASO delivery by NP is a promising therapeutic modality providing stability of the encapsulated ASOs and a sustained release. These drugs differ from small-molecule pharmaceuticals in that instead of binding to a pocket of the protein to block certain activities, they prevent the protein from being expressed altogether. This minimizes side effects, and increases the effectiveness of the drug.

8. Refined method for tumor cell application and – detection

The basic procedures used for anesthesia and tumor cell implantation were as described above (see chapter 2) except for the following aspects:
Subsequently to preparing the femoral artery as well as their related arteries (saphenous artery, popliteal artery, descending genicular artery, superficial epigastric artery), they were freed from the surrounding fat tissue and mobilized (Fig. 8a, b).

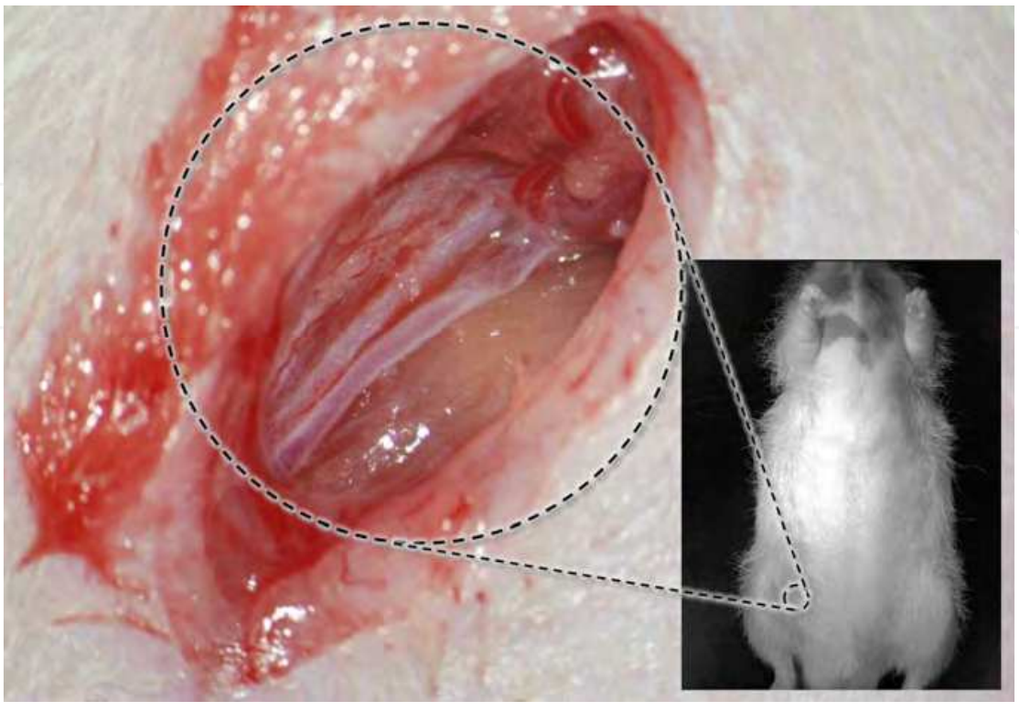

Fig. 8a. Region prepared for tumor cell implantation.

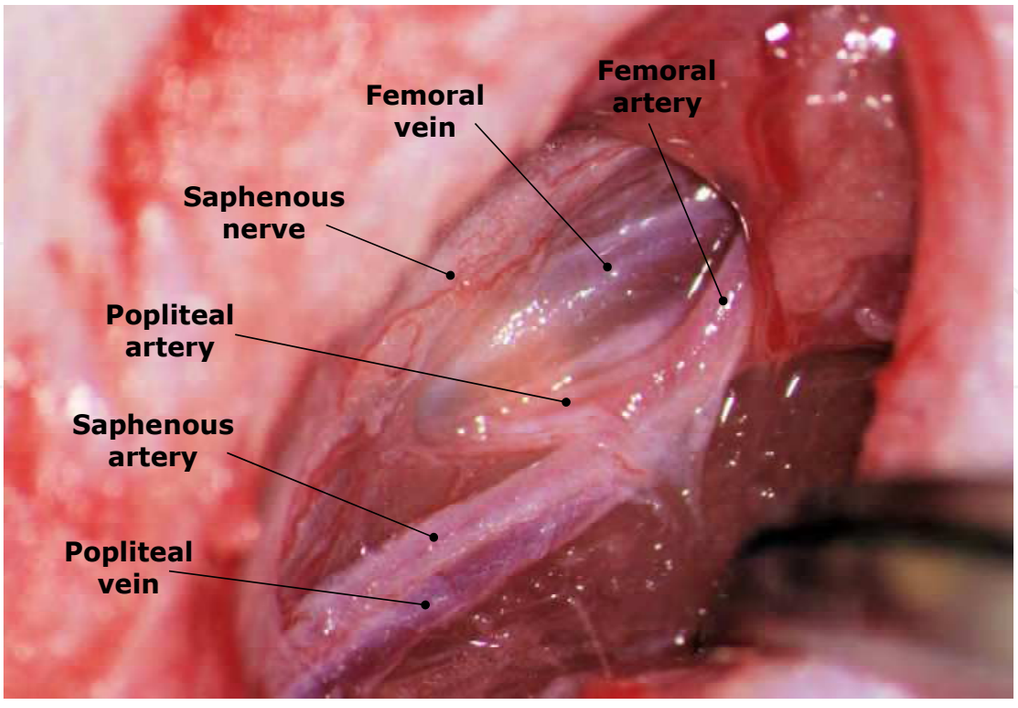

Fig. 8b. Mobilized arterial branches.

Then the femoral artery was separated from the neighboring vein and -nerve in the area in which the saphenous and superficial epigastric arteries branch off the femoral artery. These vessels were exposed to a 1% papaverin solution to inhibit their contraction. After an incubation time of one minute, the femoral artery as well as the saphenous and popliteal arteries were temporarily occluded by ligating them with three surgical threads (Prolene 7-0, Ethicon) (Fig. 9).

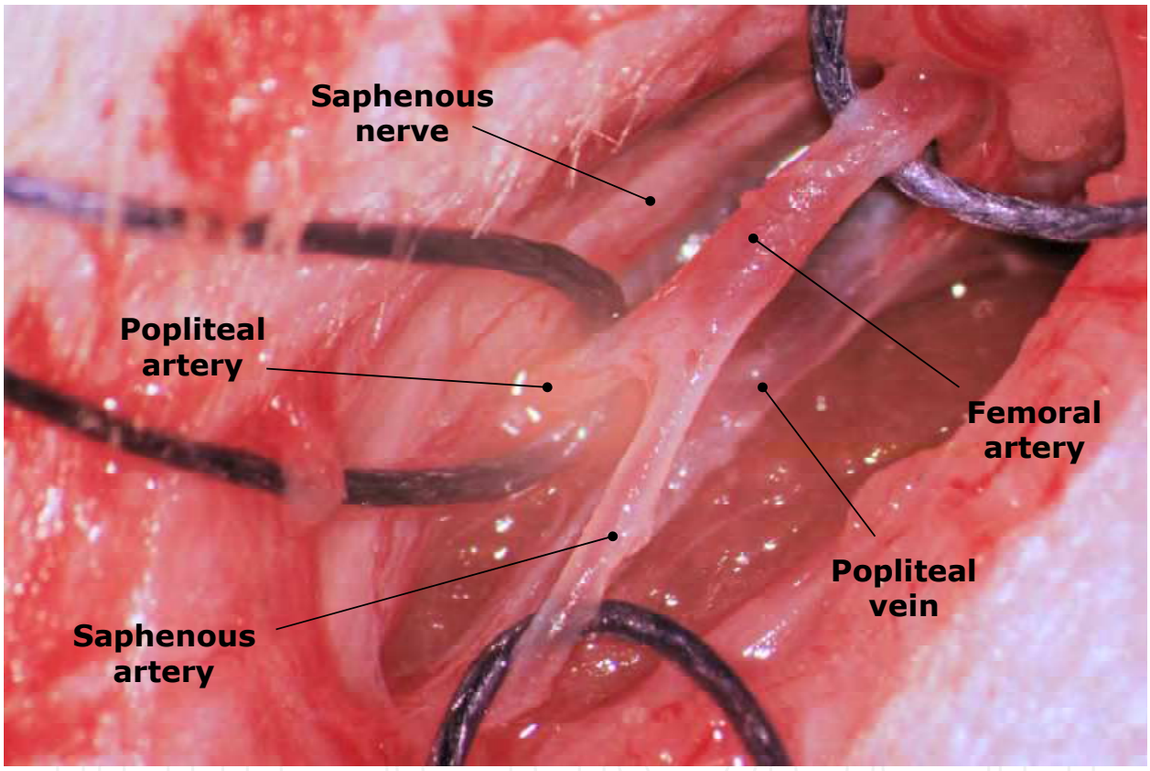

Fig. 9. Arterial branches prepared for tumor cell injection.

This enabled to control the blood flow as well as the direction of inoculated tumor cells. To that purpose a cannula (27G x ½") was inserted into the dilated lumen of the saphenous artery. Due to the persisting blockade of the femoral and saphenous arteries the tumor cells ($1x10^5$ cells in 0.2 ml PBS) and the blood stream were directed only into the popliteal artery (Fig. 10a, b).

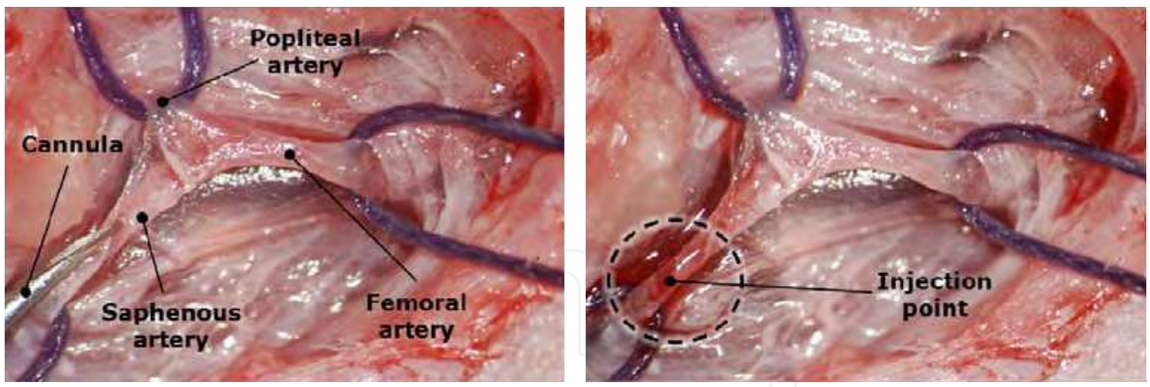

Fig. 10. a. Placement of the cannula into the saphenous arterty, b. Puncture site after withdrawal of the cannula.

For better visualization, trypan blue was injected to demonstrate the successful direction of the injected volume by the colored vessel walls (Fig. 11 a). After withdrawal of the cannula, the perforation of the arterial wall was sealed by using a piece of fat tissue which was pressed on the puncture site by sterile cotton swabs until the bleeding halted (Fig. 11. b). Subsequently, the operation site was closed as described above.

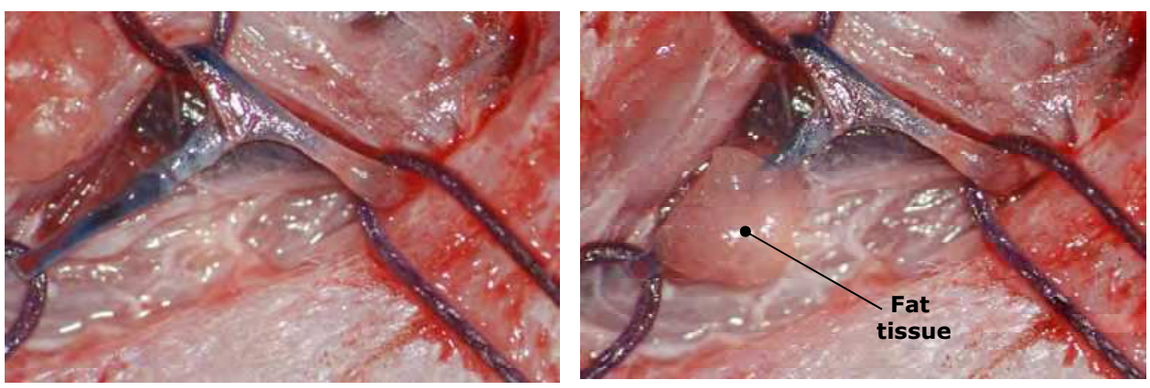

Fig. 11. a. Colored vessel walls show the direction of the blood stream, b. the puncture site has been closed by fat tissue.

Advantage of the refined method for tumor cell application.
The refined method allows to re-use the same artery after tumor cell injection, e.g. for locally administering therapeutics. In addition, it qualifies by a smaller surgical wound and a reduced time required for the surgical procedure.
Both methods result in the loco-regional application of tumor cells causing local tumor growth, only. The resulting osteolytic lesions caused in femur, tibia and fibula of the corresponding hind leg can be monitored by CT as early as two to four weeks after tumor cell implantation. In addition, the soft tissue tumor can be recorded by MRT for lesions ≥ 1 mm^3 (corresponding to 1 x 10^6 tumor cells). The need to observe disease progression of tumor cells in animal models has led to the development of various imaging techniques.
For monitoring the state of tumor cells directly after their intra-femoral application, the tumor cells have been stably transfected with the reporter genes (firefly-) luciferase and

(cherry-) RFP. The luciferase marker gene allows a non-invasive detection of tumor cells down to 1 x 10^3 tumor cells per hind leg (Fig. 12 a, b).
The intraperitoneal injection of luciferin (500 µl of a potassium-D-luciferin solution (1.5mg/rat)) results in a light emission which can be detected by a sensitive CCD camera (IVIS Imaging System – Series 100).

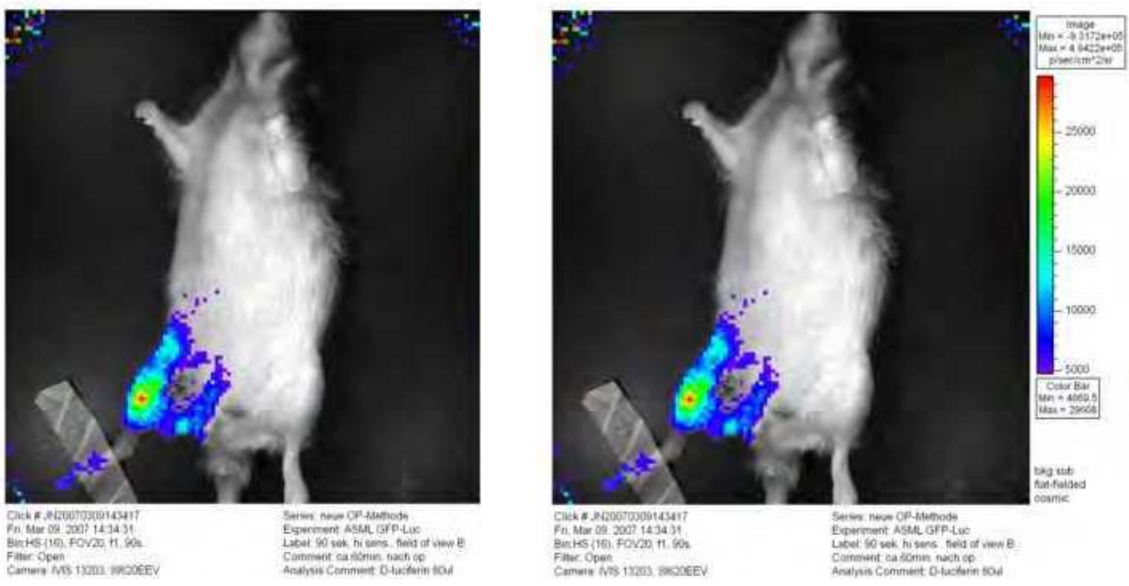

Fig. 12. a. 10 Minutes after implantation of 1 x 105 tumor cells and injection of 1.5 mg luciferin, b. 60 Minutes after implantation of 1 x 105 tumor cells and re-injection of 1.5 mg luciferin.

Bioluminescence Imaging (BLI) is an extremely sensitive method for detecting metastases. Already micro-metastatic signals from a few thousand luciferase positive MDA-MB-$231^{RFP/Luci+}$ cells were detectable. However, a crucial drawback of the bioluminescence method is the relatively poor spatial resolution and the fact that luciferase-transfected cells are indispensably needed. A comparison of the three methods for cell monitoring and their sensitivities is given in Figure 13.

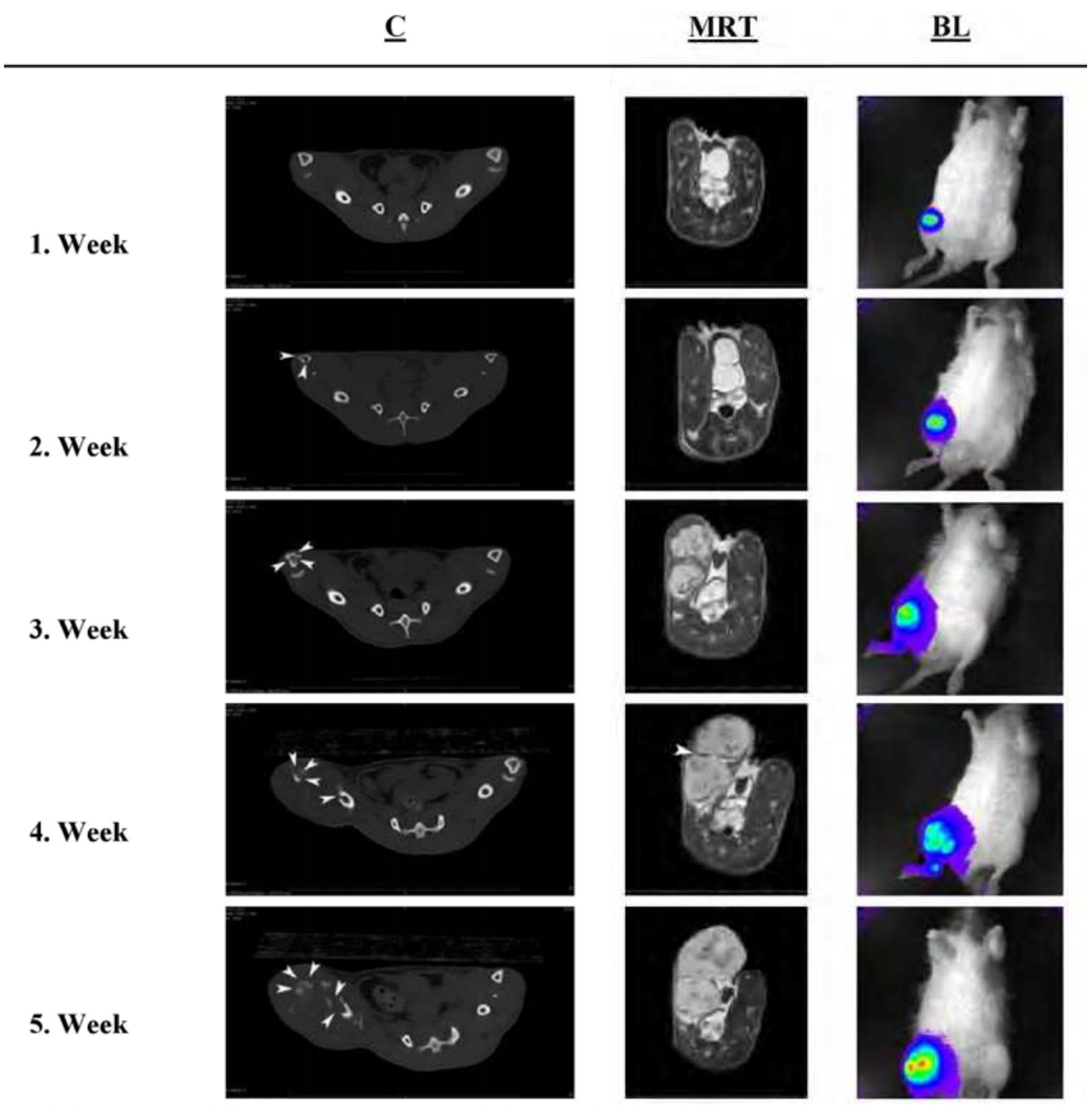

Fig. 13. Comparison of three different methods for monitoring lytic lesions of an untreated control rat.
CT: Bone lesions were detected two weeks after tumor cell injection. Owing to contrast, bone can be differentiated from soft tissues like muscles or fat. As for MRT, a three dimensional reconstruction can be generated. However, there is exposure to radiation and this technique as well as MRT is distinctly more complex and expensive than BLI.
MRT: One advantage of this method is the possibility to measure the volume of the lesions. Another advantage is related to the high contrast found for soft tissues, including their pathologic alterations. This is due to an extremely high resolution.
BLI: As soon as one week after inoculation the MDA-MB231-cells were detected by light emission in response to luciferin administration. With time, the signal increased in size regarding the emitting area as well as its intensity. BLI was the most sensitive method for detecting bone metastases.

9. Acknowledgments

These studies were supported in part by the BMBF BioDisc Cooperation (DKFZ-MOS), Grant No. 0315014/G401 as well as by the company Immundiagnostik AG, Wiesenstrasse 4, 64525 Bensheim, Germany.

10. References

[1] Guise TA: Molecular mechanisms of osteolytic bone metastases. Cancer 88 (Suppl 12): 2892-2898, 2000.
[2] Coleman RE: Skeletal complications of malignancy. Cancer 80 (Suppl 8): 1588-1594, 1997.
[3] Clohisy DR and Mantyh PW: Bone cancer pain. Cancer 97 (Suppl 3): 866-873, 2003.
[4] Withold W, Armbruster FP, Karmatschek M and Reinauer H: Bone sialoprotein in serum of patients with malignant bone diseases. Clin Chem 43: 85-91, 1997.
[5] Bellahcene A, Antoine N, Clausse N, Tagliabue E, Fisher LW, Kerr JM, Jares P and Castronovo V: Detection of bone sialoprotein in human breast cancer tissue and cell lines at both protein and messenger ribonucleic acid levels. Lab Invest 75: 203-210, 1996.
[6] Diel IJ, Solomayer EF, Seibel MJ, Pfeilschifter J, Maisenbacher H, Gollan C, Pechterstorfer M, Conradi R, Kehr G, Boehm E, Armbruster FP and Bastert G: Serum bone sialoprotein in patients with primary breast cancer is a prognostic marker for subsequent bone metastasis. Clin Cancer Res 5: 3914-3919, 1999.
[7] Fedarko NS, Jain A, Karadag A, van Eman MR and Fisher LW: Elevated serum bone sialoprotein and osteopontin in colon, breast, prostate, and lung cancer. Clin Cancer Res 7: 4060-4066, 2001.
[8] Bellahcene A, Menard S, Bufalino R, Moreau L and Castronovo V: Expression of bone sialoprotein in primary human breast cancer is associated with poor survival. Int J Cancer 69: 350-353, 1996.
[9] Ibrahim T, Leong I, Sanchez-Sweatman O, Khokha R, Sodek J, Tenenbaum HC, Ganss B and Cheifetz S: Expression of bone sialoprotein and osteopontin in breast cancer bone metastases. Clin Exp Metastasis 18: 253-260, 2000.
[10] Waltregny D, Bellahcene A, De Leval X, Florkin B, Weidle U and Castronovo V: Increased expression of bone sialoprotein in bone metastases compared with visceral metastases in human breast and prostate cancers. J Bone Miner Res 15: 834-843, 2000.
[11] Carlinfante G, Vassiliou D, Svensson O, Wendel M, Heinegard D and Andersson G: Differential expression of osteopontin and bone sialoprotein in bone metastasis of breast and prostate carcinoma. Clin Exp Metastasis 20: 437-444, 2003.
[12] Fisher LW, Torchia DA, Fohr B, Young MF and Fedarko NS: Flexible structures of SIBLING proteins, bone sialoprotein, and osteopontin. Biochem Biophys Res Commun 280: 460-465, 2001.
[13] Fisher LW, Jain A, Tayback M and Fedarko NS: Small integrin binding ligand N-linked glycoprotein gene family expression in different cancers. Clin Cancer Res 10: 8501-8511, 2004.
[14] Ganss B, Kim RH and Sodek J: Bone sialoprotein. Crit Rev Oral Biol Med 10: 79-98, 1999.
[15] Fisher LW, Whitson SW, Avioli LV and Termine JD: Matrix sialoprotein of developing bone. J Biol Chem 258: 12723-12727, 1983.

[16] Bianco P, Fisher LW, Young MF, Termine JD and Robey PG: Expression of bone sialoprotein (BSP) in developing human tissues. Calcif Tissue Int 49: 421-426, 1991.
[17] Tye CE, Hunter GK and Goldberg HA: Identification of the type I collagen-binding domain of bone sialoprotein and the mechanism of interaction. J Biol Chem 280: 13487-13492, 2005.
[18] Ross FP, Chappel J, Alvarez JI, Sander D, Butler WT, Farach-Carson MC, Mintz KA, Robey PG, Teitelbaum SL and Cheresh DA: Interactions between the bone matrix proteins osteopontin and bone sialoprotein and the osteoclast integrin alpha v beta 3 potentiate bone resorption. J Biol Chem 268: 9901-9907, 1993.
[19] Somerman MJ, Fisher LW, Foster RA and Sauk JJ: Human bone sialoprotein I and II enhance fibroblast attachment in vitro. Calcif Tissue Int 43: 50-53, 1988.
[20] Fedarko NS, Fohr B, Robey PG, Young MF, Fisher LW: Factor H binding to bone sialoprotein and osteopontin enables tumor cell evasion of complement-mediated attack. J Biol Chem. 2000 Jun 2; 275(22):16666-72.
[21] Rudland PS, Platt-Higgins A, El-Tanani M, et al. (2002): Prognostic significance of the metastasis-associated protein osteopontin in human breast cancer. Cancer Res.; 62:3417–3427.
[22] Tuck AB, Chambers AF (2001): The role of osteopontin in breast cancer: Clinical and experimental studies. J Mammary Gland. Biol Neoplasia. 6:419–427.
[23] Senger DR, Perruzzi CA and Papadopoulos A: Elevated expression of secreted phosphoprotein I (osteopontin, 2ar) as a consequence of neoplastic transformation. Anticancer Res 9: 1291-1299, 1989.
[24] Barry ST, Ludbrook SB, Murrison E and Horgan CM: Analysis of the alpha4beta1 integrin-osteopontin interaction. Exp Cell Res 258: 342-351, 2000.
[25] Smith LL and Giachelli CM: Structural requirements for alpha 9 beta 1-mediated adhesion and migration to thrombin-cleaved osteopontin. Exp Cell Res 242: 351-360, 1998.
[26] Weber GF: The metastasis gene osteopontin: a candidate target for cancer therapy. Biochim Biophys Acta: 1552: 61-85, 2001.
[27] Rosol TJ, Tannehill-Gregg SH, LeRoy BE, Mandl S, Contag CH (2003): Animal models of bone metastasis. Cancer; 97:748–57.
[28] Rogers MJ, Watts DJ, Russell RGG (1997): Overview of bisphosphonates. Cancer 80(8):1652–1660.
[29] Green JR (2002): Bisphosphonates in cancer therapy. Current opinion in oncology: 14:609–615.
[30] Green JR (2003): Antitumor effects of bisphosphonates. Cancer 97(3Suppl):840–847.
[31] Ross JR, Saunders Y, Edmonds PM, Patel S, Broadley KE, Johnston SRD (2003): Systematic review of role of bisphosphonates on skeletal morbidity in metastatic cancer. BMJ 327:469.
[32] Yoneda T, Michigami T, Bing Y, Williams PJ, Niewolna M, Hiraga T (2000): Actions of bisphosphonate on bone metastasis in animal models of breast carcinoma. Cancer 88:2979–2988
[33] Hiraga T, Ueda A, Tamura D, Hata K, Ikeda F, Williams PJ, Yoneda T (2003): Effects of oral UFT combined with or without zoledronic acid on bone metastasis in the 4T1/luc mouse breast cancer. Int J Cancer 106:973–979.
[34] Bäuerle T, Adwan H, Kiessling F, Hilbig H, Armbruster FP, Berger MR (2005): Characterization of a rat model with sitespecific bone metastasis induced by MDA-MB-231 breast cancer cells, and its application to the effects of an antibody against bone sialoprotein. Int J Cancer 115:177–186.

[35] Bäuerle T, Peterschmitt J, Hilbig H, Kiessling F, Armbruster FP, Berger MR (2006): Treatment of bone metastasis induced by MDA-MB-231 breast cancer cells with an antibody against bone sialoprotein. Int J Oncology 28:573–583.
[36] Adwan H, Bäuerle TJ, Berger MR. (2004): Downregulation of osteopontin and bone sialoprotein II is related to reduced colony formation and metastasis formation of MDA-MB-231 human breast cancer cells. Cancer Gene Ther; 11:109–20.
[37] Adwan H, Bäuerle TJ, Najajreh Y, Elazer V, Golomb G, Berger MR (2004): Decreased levels of osteopontin and bone sialoprotein II are correlated with reduced proliferation, colony formation, and migration of GFP-MDA-MB-231 cells. Int J Oncology 24: 1235-1244.
[38] Kakonen SM, Mundy GR (2003): Mechanisms of osteolytic bone metastases in breast carcinoma. Cancer; 97:834–9
[39] Mundy GR. et al. (1997): Mechanisms of bone metastasis. Cancer; 80:1546–56.
[40] Mundy GR. et al. (2002): Metastasis to bone: causes, consequences and therapeutic opportunities. Nat Rev Cancer; 2:584–93.
[41] Akhtar S, Juliano RL (1992): Cellular uptake and intracellular fate of antisense oligonucleotides. Trends Cell Biol; 2:139–44.
[42] Patil SD, Rhodes DG, Burgess DJ: DNA-based therapeutics and DNA delivery systems: a comprehensive review. AAPS J 2005; 7:E61–E77.
[43] Kurreck J. et al. (2003): Antisense technologies. Improvement through novel chemical modifications. Eur J Biochem; 270:1628–44.
[44] Mahato RI, Takakura Y, Hashida M (1997): Development of targeted delivery systems for nucleic acid drugs. J Drug Target; 4:337–57.
[45] Smith AE (1995): Viral vectors in gene therapy. Annu Rev Microbiol; 49:807–38.
[46] Ledley FD et al. (1994): Non-viral gene therapy. Curr Opin Biotechno; 5:626–36.
[47] Zhang L, Gu FX, Chan JM, Wang AZ, Langer RS, Farokhzad OC (2008): Nanoparticles in medicine: therapeutic applications and developments. Clin Pharmacol Ther; 83:761–9.
[48] Li SD, Huang L (2008): Pharmacokinetics and biodistribution of nanoparticles. Mol Pharm; 5:496–504.
[49] Shive MS, Anderson JM (1997): Biodegradation and biocompatibility of PLA and PLGA microspheres. Adv Drug Deliv Rev; 28:5–24.
[50] Cohen H, Levy RJ, Gao J, Fishbein I, Kousaev V, Sosnowski S, Slomkowski S, Golomb G (2000): Sustained delivery and expression of DNA encapsulated in polymeric nanoparticles. Gene Ther; 7: 1896–905.
[51] Cohen-Sacks H, Najajreh Y, Tchaikovski V, Gao G, Elazer V, Dahan R, Gati I, Kanaan M, Waltenberger J, Golomb G (2002): Novel PDGFbetaR antisense encapsulated in polymeric nanospheres for the treatment of restenosis. Gene Ther; 9:1607–16.
[52] Elazar V., Adwan H, Rohekar K, Zepp M, Lifshitz-Shovali R, Berger MR, Golomb G: Biodistribution of antisense nanoparticles in mammary carcinoma rat model. Drug Delivery, 2010, 1–11, Early Online
[53] Elazar V., Adwan H, Bäuerle TJ, Rohekar K, Golomb G, Berger MR (2010): Sustained delivery and efficacy of polymeric nanoparticles containing osteopontin and bone sialoprotein antisenses in rats with breast cancer bone metastasis. Int J Cancer; 126(7):1749-60.
[54] Bishop JS, Guy-Caffey JK, Ojwang JO, Smith SR, Hogan ME, Cossum PA, Rando RF, Chaudhary N. (1996): Intramolecular G-quartet motifs confer nuclease resistance to a potent anti-HIV oligonucleotide. J Biol Chem; 271:5698–703.

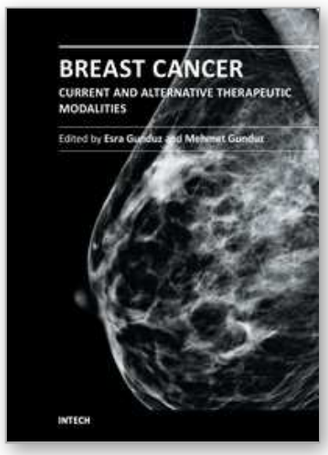

Breast Cancer - Current and Alternative Therapeutic Modalities
Edited by Prof. Esra Gunduz

ISBN 978-953-307-776-5
Hard cover, 540 pages
Publisher InTech
Published online 09, November, 2011
Published in print edition November, 2011

Cancer is the leading cause of death in most countries and its consequences result in huge economic, social and psychological burden. Breast cancer is the most frequently diagnosed cancer type and the leading cause of cancer death among females. In this book, we discussed various therapeutic modalities from signaling pathways through various anti-tumor compounds as well as herbal medicine for this deadly cancer. We hope that this book will contribute to the development of novel diagnostic as well as therapeutic approaches.

INTECH
open science | open minds

InTech Europe
University Campus STeP Ri
Slavka Krautzeka 83/A
51000 Rijeka, Croatia
Phone: +385 (51) 770 447
Fax: +385 (51) 686 166
www.intechopen.com

InTech China
Unit 405, Office Block, Hotel Equatorial Shanghai
No.65, Yan An Road (West), Shanghai, 200040, China
中国上海市延安西路65号上海国际贵都大饭店办公楼405单元
Phone: +86-21-62489820
Fax: +86-21-62489821

IntechOpen